A Simple and Reliable Method for Gas Well Deliverability Determination

Arman G. Yussefabad

Thesis submitted to the
College of Engineering and Mineral Resources
at West Virginia University
in Partial Fulfillment of the Requirements
for the Degree of

Master of Science
In
Petroleum and Natural Gas Engineering

Dr. Khashayar Aminian, Chair
Professor Samuel Ameri
Dr. Shahab Mohaghegh

Department of Petroleum and Natural Gas Engineering

Morgantown, West Virginia
2007

Keywords: Inertial coefficient, Deliverability Equation, Non-Darcy Coefficient, Skin Factor, Permeability

ABSTRACT

A Simple and Reliable Method for Gas Well Deliverability Determination

Arman G. Yussefabad

Multi-rate tests generally provide accurate values for gas reservoir formation parameters and deliverability equation coefficients. This type of results enables the engineer to make proper decisions on whether remedial work is required and the potential improvement that can be achieved. The multi-rate tests, such as isochronal or modified isochronal tests, are however cumbersome to conduct due to need for achieving stabilization or lengthy shut-in periods.

The goal of this study has been to develop a simple and reliable method for gas well deliverability determination based on a single rate build-up or fall-off test. Traditionally, single rate well tests have been analyzed using empirical backpressure equation using an average value for the exponent (n). Such approximations often provide inaccurate results and do reveal any information regarding the conditions of the well. To accurately estimate mechanical skin factor and the deliverability equation coefficients from a single rate test, turbulence factor, β, must be estimated. There are numerous correlations in the literature for estimating β. These correlations do not provide unique results and calculated skin factor can range widely as a result.

This study introduces the concept of the reservoir-specific β-factor. The methodology for developing a correlation for β factor using multi-rate tests has been developed. Once the β-factor correlation for a reservoir is established, there would be no need for multi-rate tests and single rate can be analyzed to provide accurate estimates of mechanical skin factor and deliverability equation coefficients. The accuracy of the developed

methodology has been verified through application in two separate reservoirs in the Appalachian Basin.

ACKNOWLEDGEMENTS

I would like to express my gratitude and appreciation to my academic advisor and professor, Dr. Kashy Aminian, for his patience, guidance, and supervision during my graduate program. His support and belief always guided my work and made achievable what was perceived as a distant dream. I would also like to thank Professor Sam Ameri for his continued encouragement and motivation during my stay at West Virginia University. I appreciate your participation and enthusiasm to be part of my committee. I would like to thank Professor Dr, Shahab Mohaghegh for his involvement in my committee. I dedicate my work to my parents, my brothers and sisters, for their unconditional love and support. I share all my accomplishments with them, it has been an aspiration of mine for sometime to complete my degree, and I thank them for believing in me. Last but not the least; I would like to thank my friends, Tracey Ford, Ken Ashtari, Bijan Bahramrad, Ali Afshar, and Ali Ghafori for all their support.

TABLE OF CONTENTS

ABSTRACT ii

ACKNOWLEDGMENTS iv

LIST OF TABLES vii

LIST OF FIGURES viii

NOMENCLATURE ix

CHAPTER 1: INTRODUCTION 1

CHAPTER 2: LITERATURE REVIEW 2

2.1 Introduction 2

2.2 Non-Darcy Flow 2

2.3 β-Correlations 3

2.4 Tortuosity Effect on Inertial Coefficient 9

2.5 Gas Well Deliverability 10

2.6 Gas Well Tests 11

2.6.1 Deliverability Tests 11

2.6.2 Pressure-Transient Tests 15

2.7 Infinite-Acting and Pseudo-Steady State Solution 16

2.8 Multi-Rate Tests Analysis 19

2.8.1 Deliverability Tests 19

2.8.2 Pressure-Transient Tests Analysis 20

CHAPTER 3: OBJECTIVE & METHODOLOGY 23

3.1 Description 23

3.2 Well Test Data Collection and Analysis 24

3.2.1 Reservoir *A* Description 24

3.2.2 Reservoir *B* Description 25

3.2.3 Multi-Rate Test Analysis 26

3.3 Evaluation of the Existing β Correlations 27

3.3.1 Evaluation of the Existing β Correlations for Wells in Reservoir *A* 27

3.3.2 Evaluation of the existing β correlations for wells in reservoir *B* 28

3.4 Proposed Methodology to Predict Gas Well Deliverability 29

3.5 Developing Reservoir-Specific β Correlation and Verification 30

3.5.1 Reservoir *A* 30
3.5.2 Reservoir *B* 31
CHAPTER 4: RESULTS & DISCUSSION 32
CHAPTER 5: CONCLUSIONS & RECOMMENDATIONS 40
REFRENCES 42
APPENDIX A 48
APPENDIX B 56
APPENDIX C 69
APPENDIX D 77

LIST OF TABLES

Table 2.1: Constant *a* and *b* in Cook's equation 4
Table 2.2: Constant *a′* and *b′* in Cook's equation 5
Table 2.3: Experimental β correlations 8
Table 3.1: Parameters used for reservoir *A* 25
Table 3.2: Parameters used for reservoir *B* 26
Table 3.3: β correlations evaluation for well 3946 and flow rate 1363.1 Mscf 28
Table 3.4: β correlations evaluation for well 7772 and flow rate 2750 Mscf 29
Table 4.1: Drawdown test analysis results for wells in reservoir *A* 32
Table 4.2: Drawdown test analysis results for wells in reservoir *B* 32
Table 4.3: β correlations evaluation for well 3946 and flow rate 2002.64 Mscf 33
Table 4.4: β correlations evaluation for well 7772 and flow rate 5203 Mscf 34
Table 4.5: Comparison of β from 2 methods 36
Table 4.6: Comparison of *s* from 2 methods, reservoir *A* 37
Table 4.7: Comparison of β from 2 methods 38
Table 4.8: Comparison of *s* from 2 methods, reservoir *B* 39
Table 4.9: Comparison of β from test and Equation (5) 39
Table A.1: Drawdown tests data for well 3585 48
Table A.2: Drawdown tests data for well 3946 49
Table A.3: Drawdown tests data for well 3827 50
Table A.4: Drawdown tests data for well 3931 51
Table A.5: Drawdown tests data for well 3870 52
Table A.6: Drawdown tests data for well 9096 53
Table A.7: Falloff test data for well 9096 53
Table A.8: Drawdown tests data for well 7772 54
Table A.9: Falloff test data for well 7772 54
Table A.10: Drawdown tests data for well 6065 55
Table A.11: Falloff test data for well 6065 55
Table B.1: Gas properties at 75 º F for well 3585 56
Table B.2: Gas properties at 75 º F for well 3946 58
Table B.3: *k* and *S'* for well 3946 58
Table B.4: *D* and *s* for well 3946 58
Table B.5: Gas properties at 75 º F for well 3827 59
Table B.6: *k* and *S'* for well 3827 59
Table B.7: *D* and *s* for well 3827 60
Table B.8: Gas properties at 75 º F for well 3931 60
Table B.9: *k* and *S'* for well 3931 61
Table B.10: *D* and *s* for well 3931 61
Table B.11: Gas properties at 75 º F for well 3870 61
Table B.12: *k* and *S'* for well 3870 62
Table B.13: *D* and *s* for well 3870 62
Table B14: Gas properties at 79 º F for well 9096 62
Table B.15: *k* and *S'* for well 9096 64
Table B.16: *D* and *s* for well 9096 64
Table B.17: Gas properties at 76 º F for well 7772 64
Table B.18: *k* and *S'* for well 7772 66
Table B.19: *D* and *s* for well 7772 66
Table B.20: Gas properties at 77 º F for well 6065 66
Table B.21: *k* and *S'* for well 6065 68
Table B.22: *D* and *s* for well 6065 68
Table C.1: β correlations evaluation for well 3585 and flow rate 2320.43 Mscf 69
Table C.2: β correlations evaluation for well 3946 and flow rate 1363.1 Mscf 70

Table C.3: β correlations evaluation for well 3827 and flow rate 1171 Mscf 70
Table C.4: β correlations evaluation for well 3931 and flow rate 2082.39 Mscf 71
Table C.5: β correlations evaluation for well 3870 and flow rate 1639.57 Mscf 71
Table C.6: β correlations evaluation for well 9096 and flow rate 350 Mscf 72
Table C.7: β correlations evaluation for well 7772 and flow rate 3400 Mscf 72
Table C.8: β correlations evaluation for well 6065 and flow rate 2302 Mscf 73
Table C.9: k and β for wells in reservoir *A* 73
Table C.10: Comparison of β from 2 methods 74
Table C.11: k and β for wells in reservoir *B* 75
Table C.12: Comparison of β from 2 methods 76

LIST OF FIGURES

Figure 2.1: Pressure and flow rate history of a typical flow-after-flow test 12
Figure 2.2: Pressure and flow rate history of a typical isochronal test 14
Figure 2.3: Pressure and flow rate history of a typical modified isochronal test 15
Figure 2.4: Analysis of Data-Houpeurt method for flow after flow test 19
Figure 3.1: Log-log plot of permeability vs. inertial coefficient for reservoir *A* using five wells 31
Figure 4.1: Log-log plot of *K* versus β for reservoir *A* using only 4 wells 35
Figure 4.2: Log-log plot of permeability vs. inertial coefficient for reservoir *A* using only 5 wells 36
Figure 4.3: Log-log plot of permeability vs. inertial coefficient for reservoir *B* using 3 wells 38
Figure B.1: Drawdown log-log plot for well 3585, q = 1301.34 Mscf 56
Figure B.2: Drawdown semi-log plot for well 3585, q = 1301.34 Mscf 57
Figure B.3: Drawdown semi-log plot for well 3946, q = 1363.1 Mscf 58
Figure B.4: Drawdown semi-log plot for well 3827, q = 308.32 Mscf 59
Figure B.5: Drawdown semi-log plot for well 3931, q = 820.19 Mscf 60
Figure B.6: Drawdown semi-log plot for well 3870, q = 942.43 Mscf 61
Figure B.7: Drawdown test semi-log plot for well 9096, q = 350 & 430 Mscf 62
Figure B.8: Falloff test, semi-log plot for well 9096 63
Figure B.9: Drawdown semi-log plot for well 7772, q = 2750, 3400 and 5203 Mscf 65
Figure B.10: Falloff test semi-log plot for well 7772 65
Figure B.11: Drawdown semi-log plot for well 6065, q = 1450, 1749 and 2302 Mscf 67
Figure B.12: Falloff test semi-log plot for well 6065 67

NOMENCLATURE

ν = Velocity (ft/hr)

q = Flow rate (MSCF/D)

S = Skin factor

S` = Apparent skin factor

k = Permeability (md)

t = Time (Hrs)

ϕ = Porosity (%)

μ_i = Initial gas viscosity (cp)

$\overline{\mu}$ = Average gas viscosity (cp)

c_{ti} = Initial gas compressibility (psia $^{-1}$)

$m(\overline{p}_R)$ = Reservoir pseudo-pressure (psia^2/ cp)

m(P)= Reservoir pseudo-pressure (psia^2/ cp)

P_p (P) = Reservoir pseudo-pressure (psia^2/ cp)

r_w= Wellbore radius (ft)

h = Net pay thickness (ft)

m = slope (psia/cycle)

A = Deliverability coefficient

B = Deliverability coefficient

c_t = Total compressibility (psi^{-1})

h= Formation thickness (ft)

k = Permeability (md)

p= Pressure (psia)

q = Production rate (Mscf/d)

r_e =Rreservoir radius(ft)

t = Time (hr)

T = Reservoir temperature ($^{\circ}$R)

Z = Gas deviation factor

L = Core length

L_a = Actual flow path

a = constant

b = constant

a' = constant

b' = constant

C = constant

n = constant

Greek symbols

ρ = Fluid density (lbm/ft^3)

β = Non-Darcy flow coefficient (ft^{-1})

φ = Porosity

γ_g = Specific gas gravity

μ = Viscosity (cp)

τ = Tortuosity

Subscripts and superscripts

i = Initial

w = Wellbore

w_f = Flowing wellbore

R = Reservoir

p = Production

a = Adjusted

CHAPTER 1

INTRODUCTION

The deliverability of well is a very essential tool to determine well capabilities to produce. Gas well deliverability is potential capabilities of well to produce gas, and it must be determined for various purposes in oil and gas industry. In order to determine gas well deliverability, multi-rate tests such as deliverability tests or transient tests must be conducted due to the non-Darcy fluid effect. To determine non-Darcy fluid effect on well deliverability, at least two single-rate tests are needed.

The current and future reservoir forecast is made based on knowledge of the well deliverability. To determine a gas well deliverability equation, multi-rate tests must be conducted. The results obtained from multi-rate tests can usually provide accurate values of the well deliverability equation coefficients. Multi-rate tests are flow tests designed to measure the production capabilities of a well under specific reservoir conditions. Although these tests are used primarily for gas wells, they are applicable to oil wells as well.

Multi-rate tests are a very efficient tool to determine a well deliverability; however, conducting these tests requires a long period of time due to the shut-in period or reaching the stabilization point, making them economically inapplicable. In this study a new method will be investigated to determine well deliverability without the need for multi-rate tests.

CHAPTER 2

LITERATURE REVIEW

2.1 Introduction

In order to understand the purpose of this study better, a brief review on the movement of fluid flow in the porous medium is presented first.

2.2 Non-Darcy Flow

Darcy (1956) described the movement of fluid flow in the porous medium at low velocities. Darcy's law is mathematically stated by the following equation:

$$\frac{\Delta p}{\Delta L} = \frac{\mu v}{K} \qquad (1)$$

In most cases fluid flow is governed by Darcy's law in the porous media, but when the flow rate is very high, for an instance, near the wellbore, Darcy's law is inadequate to describe fluid flow.

Non-Darcy flow, often called turbulent flow, may occur at high gas flow velocity. Forchheimer (1901) discovered that the pressure gradient required to sustain a high flow rate through a porous medium is higher than what Darcy's equation would predict. The deviation from Darcy's equation increased with increasing flow rate. He attributed the excess gradient required, to inertial flow resistance, which is proportional to ρv^2 .The inertial coefficient, β, is defined by the Forchheimer equation, which for one-dimensional linear flow is:

$$-\frac{dp}{dL} = \frac{\mu v}{k} + 3.238\times10^{-8}\,\beta\rho v^2 \qquad (2)$$

Where:

dp/dL = flowing pressure gradient

v =fluid velocity

ρv^2 =inertial flow term

The inertial coefficient, β, has the dimension of reciprocal length. Equation (2) indicates that the pressure gradient required to sustain a given flow rate through a porous medium is greater than would be predicted by Darcy's flow equation when the term $\beta\rho v^2$ is not negligible. Rewriting Equation (2) gives:

$$-\frac{dp}{dL} = \frac{\mu v}{k}\left(1 + \frac{c_1 k \beta \rho v}{\mu}\right) \tag{3}$$

where c_1 is a constant and the right-hand term inside parentheses represents a Reynolds number (ratio of inertial to viscous forces). If Reynolds number is close to unity, then most of the flowing pressure gradient is a result of viscous flow, and Darcy's equation applies. As the Reynolds number increases, however, the inertial forces increase significantly, and the flow can no longer be modeled with Darcy's equation. We call this the non-Darcy flow effect.

2.3 β-Correlations

Many attempts have been made to relate experimental measurements of β to rock properties such as permeability and porosity. Janicek and Katz (1955) were the first ones to develop a correlation for inertial coefficient using sandstone, limestone, and dolomite cores. They proposed to use the following equation:

$$\beta = \frac{5.55 \times 10^9}{k^{1.25}\phi^{0.75}} \tag{4}$$

Where:

k= Permeability (mD)

φ = porosity

β = non-Darcy coefficient (1/ft)

Tek et al. (1962) developed a correlation for inertial coefficient, by analyzing Janicek and Katz data. The correlation they developed was as follows:

$$\beta = \frac{2.33 \times 10^{10}}{k^{1.2}} \tag{5}$$

Where:

k= Permeability (mD)

β = non-Darcy coefficient (1/ft)

Cooke (1973) investigated the non-Darcy flow for bines, reservoir oils, and gases in propped fractures and used only permeability to predict the inertial coefficient. He developed two equations as follows:

$$\beta = \frac{b}{k^{a}} \tag{6}$$

Where:

k= Fractured permeability (mD)

β = non-Darcy coefficient (1/ft)

a and *b* are constants determined by experiments based on proppant type. Table 2.1, summarizes the constant values for Cooke's equation.

Table 2.1: Constant *a* and *b* in Cook's equation

sand size (mesh)	a	b
8 to 12	1.24	3.32
10 to 20	1.34	2.63
20 to 40	1.54	2.65
40 to 60	1.6	1.10

and

$$\beta = \frac{3.05 \times 10^{7} b^{'}}{k^{a^{'}}} \tag{7}$$

Where:

k= Fractured permeability (mD)

β = non-Darcy coefficient (1/ft)

$a^{'}$ and $b^{'}$ are constants determined by experiments based on proppant type. Table 2.2 summarizes the constant values for Cooke's equation.

Table 2.2: Constant *a'* and *b'* in Cook's equation

sand size (mesh)	a'	b'
8 to 12	1.24	17423.61
10 to 20	1.34	27539.48
20 to 40	1.54	1104070.39
40 to 60	1.60	69405.31

Geertsma (1974) analyzed the data obtained from consolidated and unconsolidated sandstones, limestones, and dolomites from his experiments, and developed the following equation:

$$\beta = \frac{4.85 \times 10^{4}}{k^{0.5} \phi^{5.5}} \tag{8}$$

Where:

k= Permeability (mD)

β = non-Darcy coefficient (1/ft)

Pascal et al. (1980) proposed a mathematical model to estimate the inertial coefficient and facture length, by using the model and the data from variable rate test from low

permeability gas reservoir. The model is illustrated using several field cases from hydraulically fractured gas well. The correlation they developed was as follows:

$$\beta = \frac{1.46\times10^{12}}{k^{1.176}} \tag{9}$$

Where:

k= Permeability (mD)

β = Non-Darcy coefficient (1/ft)

Jones (1987) performed experiments on 29 limestone and 355 sandstone cores, which were in different core types: vuggy limestone, fine-grained sandstone and crystalline limestone. By analyzing the data from his experiments, he developed two correlations to estimate the inertial coefficient as follows:

$$\beta = \frac{6.15\times10^{10}}{k^{1.55}} \tag{10}$$

Where:

k= Permeability (mD)

β = non-Darcy coefficient (1/ft)

and

$$\beta = \frac{1.88\times10^{10}}{k^{1.47}\phi^{0.53}} \tag{11}$$

k= Permeability (mD)

β = non-Darcy coefficient (1/ft)

Coles and Hartman (1998) proposed a correlation for inertial coefficient by conducting their experiment on limestone and sandstone samples with the same porosity (with no liquid present) and they arrived to the following equation:

$$\beta = \frac{1.07 \times 10^{12} \phi^{0.449}}{k^{1.88}} \tag{12}$$

Where:

k= Permeability (mD)

β = non-Darcy coefficient (1/ft)

Coles and Hartman (1998) proposed another correlation for inertial coefficient base on their experiment on the sandstone and limestone (with liquid present):

$$\beta = \frac{2.49 \times 10^{11} \phi^{0.537}}{k^{1.79}} \tag{13}$$

Where:

k= Permeability (mD)

β = non-Darcy coefficient (1/ft)

Based on the theoretical equation developed by Ergun and Orning, Ergun found an empirical equation by analyzing the data from 640 experiments conducted by him, and the data he found in the literature, which involved various-size spheres, sand, pulverized coke, and the following gases: carbon dioxide, nitrogen, methane, and hydrogen. According to Thauvin and Mohant (1998), the comparison of Ergun's empirical flow equation with Forchheimer equation leads to:

$$\beta = \frac{4.36 \times 10^{4}}{k^{0.5} \phi^{1.5}} \tag{14}$$

Where:

k= Permeability (Darcy)

β = non-Darcy coefficient (1/ft)

Svec and Engler (2001) have designed a model that has been verified using laboratory high flow data obtained using single-phase nitrogen gas. The data comprised a wide range of flow rates collected using a heterogeneous Berea sandstone wafer as follows:

$$\beta = \frac{3.51\times10^{8}}{k\phi} \tag{15}$$

Where:

k= Permeability (mD)

β = non-Darcy coefficient (1/ft)

Table 2.3 summarizes the author and corresponding experimental correlation

Table 2.3: Experimental *β* correlations

Author	β, 1/cm
Janicek	$1.82\times10^{8}k^{-1.25}\phi^{-0.75}$
Pascal et al	$4.8\times10^{10}k^{-1.176}$
Coles & Hartman	$3.51\times10^{10}\phi^{0.449}k^{-1.88}$
Coles & Hartman	$8.17\times10^{9}\phi^{0.537}k^{-1.79}$
Svec & Engler	$1.15\times10^{7}\phi^{-1}k^{-1}$
Jones	$2.018\times10^{9}k^{-1.55}$
Jones	$1.88\times10^{10}\phi^{-0.53}k^{-1.47}$
Geertsma	$1.59\times10^{3}\phi^{-5.5}k^{-0.5}$
Tek et al	$7.64\times10^{8}k^{-1.72}$
Ergun & Orning	$1428.87\phi^{-1.5}k^{-0.5}$
Cooke	$3.28\times10^{-2}bk^{-a}$
Cooke	$10^{6}b'k^{-a'}$
Liu et al	$2.92\times10^{7}\tau k^{-1}\phi^{-1}$

2.4 Tortuosity Effect on Inertial oefficient

Liu et al. plotted Equation (8) developed by Geertsma against the data obtained respectively by Cornell and Katz, Evans et al, and Whitney. They found that Equation (8) was inaccurate. By considering the effect of tortuosity, τ , of the porous medium, on the non-Darcy coefficient, and by analyzing those data, they got a better regression fit correlation as follows:

$$\beta = \frac{8.9 \times 10^8 \tau}{k\phi} \tag{16}$$

Where:

k= Fractured permeability (mD)

β = non-Darcy coefficient (1/ft)

Tortuosity is the average path length that a fluid particle must travel is actually greater that the length of the core sample. The departure of a porous medium from being made up by a bundle of straight capillaries can be measured by the tortuosity coefficient, τ , which is expressed as:

$$\tau = \left(\frac{L_a}{L} \right)^2 \tag{17}$$

where L_a is the actual flow and L is the core length.

Ramey (1965), Katz (1959), Muskut (1969), described non-Darcy flow behavior near the wellbore as a rate dependent skin as follows:

$$S' = s + Dq \tag{18}$$

As Equation (18) indicates, the apparent skin factor, S', consist of true skin factor, s, and a rate dependent part, Dq. True skin factor represents formation alteration (damage or stimulation), whereas rate dependent part represents non-Darcy flow pressure drop.

Ramey suggested that the non-Darcy flow coefficient D could be estimated from:

$$D = \frac{2.22 \times 10^{-15} \gamma_g k}{\overline{\mu} h r_w} \beta \tag{19}$$

obtained by integrating the Forchheimer equation.

2.5 Gas Well Deliverability

It is important to determine gas well production capabilities under specific conditions of reservoir and bottomhole flowing pressure. Gas well deliverability has been identified by the relationship among flow rate, reservoir and bottomhole pressures. Two main equations are being used widely in oil and gas industry to determine gas well deliverability namely empirical and theoretical equations.

The standard empirical backpressure equation or the Rawlins and Schellhardt deliverability equation was presented in 1935 and is given by:

$$q = C\left(P_R^2 - P_{wf}^2\right)^n \tag{20}$$

The standard empirical equation assumes the values of C and n remain constant and are not dependent on the flow rate. This equation does not accurately predict gas well deliverability because the pressure drop that is due to the non-Darcy effect is variable and can result in significant error.

Since Equation (20) does not allow for easy application to show the effects of formation and fluid properties on the well's deliverability, therefore the quadratic form of the deliverability equation is a better choice to determine the impact of these factors on the

well's deliverability. This form of the deliverability equation is known as the theoretical or Houpeurt equation and it is given by:

$$P_R^2 - P_{wf}^2 = Aq + Bq^2 \tag{21}$$

The Houpeurt equation considers the effect of the turbulence factor on the deliverability at a given pressure differential.

2.6 Gas Well Tests

The multi-rate tests that are routinely conducted on gas wells can be grouped into two basic categories based on their main purpose. The first category, deliverability tests, includes test designed to evaluate a well's production capability. The second category, pressure-transient tests, includes tests designed to quantify important reservoir rock and fluid properties, such as average reservoir pressure, permeability and porosity, and to identify reservoir heterogeneities.

2.6.1 Deliverability Tests: Deliverability tests are flow tests designed to measure the production capabilities of a well under specific reservoir conditions. Unlike most pressure-transient tests, deliverability tests require stabilized flowing conditions for proper analysis.

Deliverability testing also generates a reservoir inflow performance relationship (IPR). The IPR curves describe the relationship between the production rate and BHFP for a specific value of reservoir pressure. The IPR can be used to evaluate gas-well current deliverability potential under a variety of surface conditions, such as production against a fixed backpressure. The IPR also can be used to forecast future production at any stage in the reservoir's life.

A Deliverability test usually requires the well to be produced at several rates. The flowing pressure at the sand face for each rate and the sand face pressure after build-up are then measured. The pressure/flow data are then used to determine or Deliverability. Common deliverability tests include flow-after-flow, isochronal, and modified isochronal and single-point tests.

Flow-after-flow tests: sometimes called four point tests, are conducted by producing the well at a series of different stabilized flow rates and measuring the stabilized BHFP at the sandface. Each different flow rate is established in succession either with or without a very short intermediate shut-in period. Typically, conventional flow-after-flow tests are conducted with a sequence of increasing flow rates; however, if stabilized flow rates are attained, the rate sequence does not affect the test. The requirement that the flowing periods be continued until stabilization is sometimes a major limitation of the flow-after-flow test, especially in low-permeability formations that take a long time to reach stabilized flowing conditions. Figure 2.1 illustrates a flow-after-flow test.

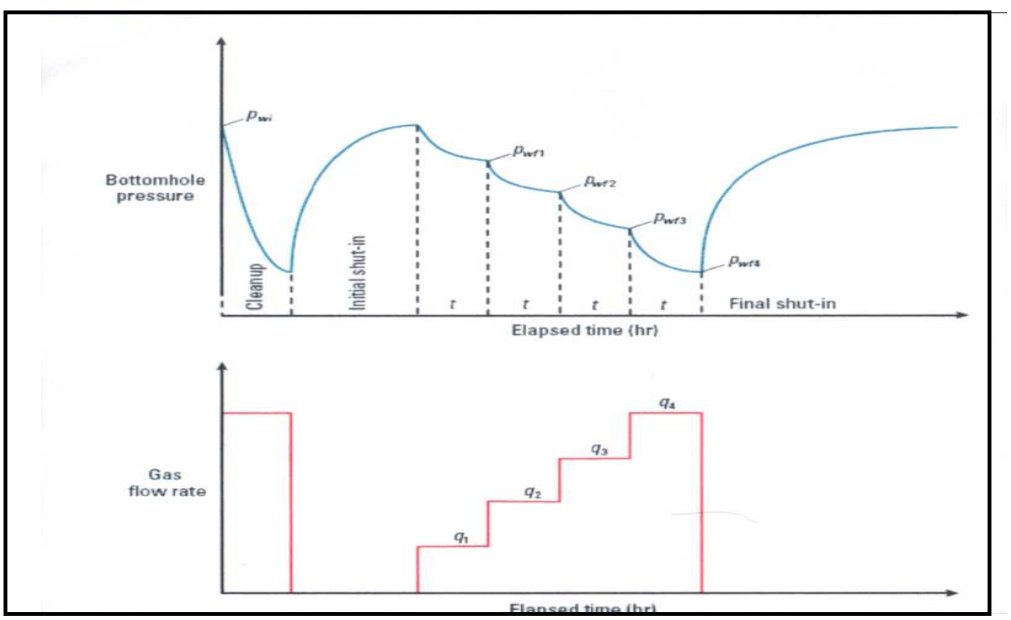

Figure 2.1: Pressure and flow rate history of a typical flow-after-flow test.

Single-point test: A single point test is an attempt to overcome the limitation of long test times required for the flow-after-flow tests in low-permeability formations. Single-point tests are conducted by flowing the well at a single rate until the BHFP is stabilized. Single-point tests are particularly appropriate when the well's deliverability characteristics are being updated. One limitation of this type of test, however, is that analysis of the results requires prior knowledge of the well's deliverability behavior. In these tests, we must ensure that the well has flowed long enough to be out of wellbore storage and in the pseudosteady-state flow regime.

Isochronal tests: Isochronal tests also were developed to shorten test times in wells that take long periods of time to stabilize. Specifically, the isochronal test is a series of single-point tests developed to estimate stabilized deliverability characteristics without actually flowing the well for the time required to achieve stabilized conditions. The isochronal test is conducted by producing and then shutting in the well and allowing it to build up to the average reservoir pressure before the next production period. Because less time is required to build up to essentially initial pressure after short flow periods than to reach stabilized flow-after-flow test, the isochronal test is more practical for low-permeability formation. Although not required for analyzing the test, a final, stabilized flow point usually is obtained at the end of the test. Figure 2.2 illustrates an isochronal test.

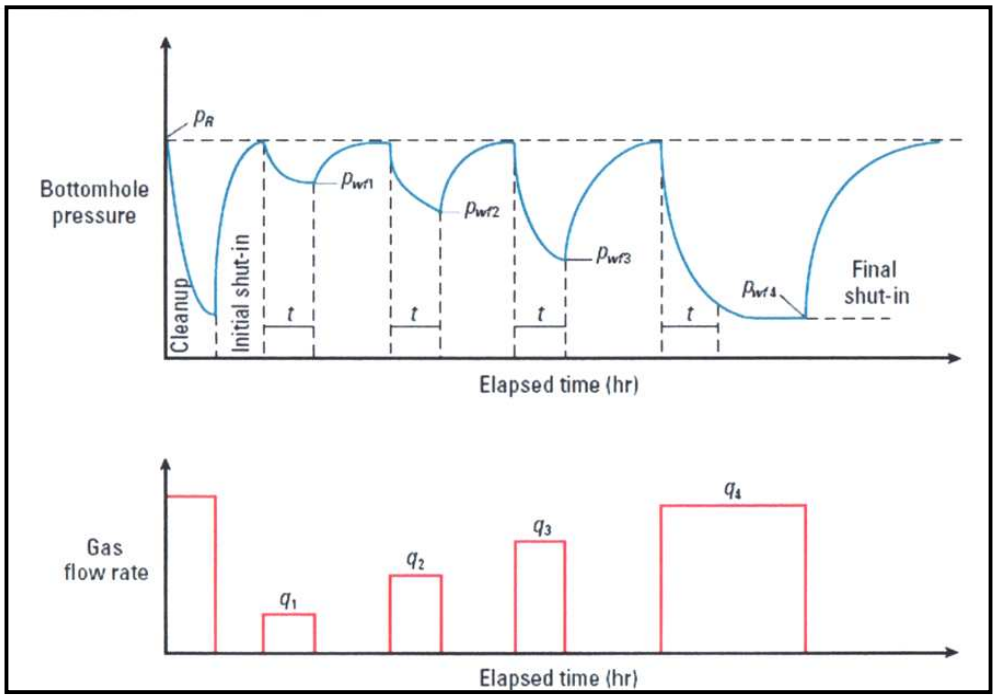

Figure 2.2: Pressure and flow rate history of a typical isochronal test.

The time to build up to the average reservoir pressure before flowing for a certain period of time may still be impractical, even after short flow periods in an isochronal test.

Modified isochronal test: In modified isochronal test, a modification of the isochronal test was developed to shorten test times further. The objective of the modified isochronal test is to obtain the same data as in an isochronal test without the sometimes lengthy shut-in periods required to reach the average reservoir pressure in the well's drainage area. The modified isochronal test is conducted like an isochronal test, except that the shut-in periods are of equal duration but should equal or exceed the length of the flow period. Note that, as the duration of the shut-in periods increases, the accuracy of the modified isochronal test also increases. Figure 2.3 illustrates a modified isochronal test.

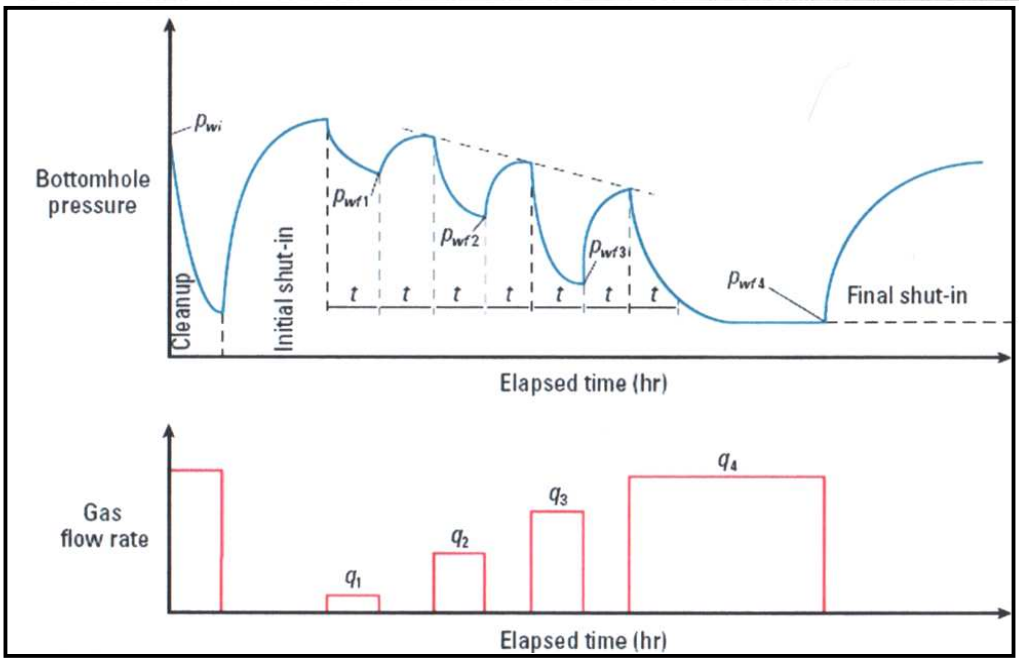

Figure 2.3: Pressure and flow rate history of a typical modified isochronal test

2.6.2 Pressure-Transient Tests: In pressure-transient tests, pressure changes are produced and recorded with respect to time. These tests enable us to evaluate not only the conditions near the wellbore area but also the reservoir properties beyond the area affected by drilling and completion operations. These well tests also can characterize important formation parameters needed to design the optimal depletion plan for the reservoir, including pressure in the drainage area of tested wells, possible presence and approximate location of flow barriers such as sealing and faults, and the dominant properties of reservoir heterogeneities such as fracture and matrix properties in a naturally fractured reservoir or individual layer properties. Pressure-transient tests can be subdivided further into single-well and multi-well tests.

Single-well tests, as the name implies, involve only one well in which the pressure response is measured following a rate change. From the measured pressure response, we

can characterize average properties in a portion or all of the drainage area of the tested well.

Drawdown test: A common pressure-transient test, drawdown or flow test, is conducted by producing a well at a known and constant rate while measuring bottomhole pressure changes as a function of time. Drawdown tests are designed primarily to quantify the reservoir flow characteristics, including permeability and skin factor. In this paper, the analysis of drawdown test has been widely used thorough out this study.

Build-up test: Another common pressure-transient test, a pressure build-up test, is performed by first stabilizing a production well at some fixed rate, placing a bottomhole pressure measuring device in the well, and shutting in the well. Following shut-in, the bottomhole pressure builds up as a function of time, and the rate of pressure buildup is used to estimate well and formation properties. Form a pressure-buildup test, we can estimate average reservoir pressure and permeability in the well drainage area and the properties of the region immediately adjacent to the wellbore.

Fall-off test: A pressure-falloff test is similar to a pressure-buildup test, except that it is conducted on an injection well. Following stabilization at some injection rate, the well is shut in. Bottomhole pressure, which begins to decrease, is measured as a function of time.

2.7 Infinite-Acting and Pseudo-Steady State Solution

In order to analyze any test to determine coefficients A and B in Equation (21), first flow regime in the reservoir must be identified. When a pressure disturbance is exerted to the system (reservoir), three flow regimes might be occurring:

1. if t π $\frac{948\phi\mu c_t r_1^2}{k}$, gas flow is in infinite-acting mode.

2. if $\frac{948\phi\mu c_t r_1^2}{k}$ π t π $\frac{948\phi\mu c_t r_2^2}{k}$, gas flow is in late transient mode.

3. if t ϕ $\frac{948\phi\mu c_t r_2^2}{k}$, gas flow is in pseudo-steady state mode.

For late transient flow regime there is no solution available, however for infinite-acting and pseudo-steady state flow regimes there is solution available as follows:

If $P < 2000$ psia , P^2 solution can be used

- Infinite-acting solution

$$P_i^2 - P_{wf}^2 = A_t q + Bq^2 \tag{22}$$

$$A_t = \frac{1637T\overline{\mu z}}{kh}\left[\log\left(\frac{kt}{\phi\overline{\mu c_t} r_w^2}\right) - 3.23 + 0.87s\right] \tag{23}$$

$$B = \frac{3.161\times10^{-12}\beta\gamma_g \overline{z}T}{r_w h^2} = \frac{1422\overline{\mu z}}{kh}D \tag{24}$$

$\overline{\mu z}$ and $\overline{\mu c}$ must be determined at $\overline{P} = \sqrt{\frac{P_i^2 + P_{wf}^2}{2}}$

- Pseudo-steady state solution

$$\overline{P}_R^2 - P_{wf}^2 = Aq + Bq^2 \tag{25}$$

$$A = \frac{1422T\overline{\mu z}}{kh}\left[\ln\left(\frac{0.427r_e}{r_w}\right) + s\right] \tag{26}$$

$$B = \frac{3.161\times10^{-12}\beta\gamma_g \overline{z}T}{r_w h^2} = \frac{1422T\overline{\mu z}}{kh}D \tag{27}$$

If $P > 2000$ psia , pseudo-pressure solution can be used

$$P_p(p) = m(p) = \Psi(p) = 2\int_0^p \frac{P'}{\mu_g(P)z(P)} dP' \tag{28}$$

$$P_p(p) = \sum_0^p \left(\frac{\overline{2P}}{\mu z} \right) \Delta P \tag{29}$$

- Pseudo-steady state solution

$$P_p\left(\overline{P_R}\right) - P_p\left(P_{wf}\right) = Aq + Bq^2 \tag{30}$$

$$A = \frac{1422T}{kh}\left[\ln\left(\frac{r_e}{r_w} \right) - 0.75 + s \right] \tag{31}$$

$$B = \frac{3.161\times10^{-12}\beta\gamma_g \bar{z}T}{r_w h^2} = \frac{1422T}{kh} D \tag{32}$$

Adjusted pressure solution can be used for all pressure range

$$P_a = \frac{\overline{\mu_g z}}{\overline{P}} \int_0^p \frac{P' \, dP'}{\mu z} \tag{33}$$

$$t_a = \left(\overline{\mu c_g}\right) \int_0^t \frac{dt'}{\mu c_g} \tag{34}$$

- If P < 2000 psi

$$\mu z = \text{constant} \approx \overline{\mu z} \quad \Rightarrow \quad P_a \approx \frac{P^2}{2\overline{P}}$$

$$\mu c_t = \text{constant} \approx \overline{\mu c_t} \quad \Rightarrow \quad t_a \approx t$$

Since reservoir and bottomhole pressures are less than 1500 psia, either pressure-square method or adjusted pressure method can be used. For simplicity pressure-square method has been used throughout this study.

2.8 Multi-Rate Tests Analysis

In order to obtain the deliverability equation (Equation 21) for each gas well, multi-rate tests must be conducted on gas well.

2.8.1 Deliverability Tests Analysis: Houpeurt method must be used to analyze deliverability tests to determine coefficients *A* and *B* in Equation (21). The procedure for Houpeurt analysis is as follows:

Plot $\dfrac{\overline{P}_s^2 - P_{wf}^2}{q}$ vs. q on the Cartesian paper

Draw the best straight line through the points

Extrapolate the line to intersect y-axis

Figure 2.4 illustrates Houpeurt analysis for flow-after-flow test.

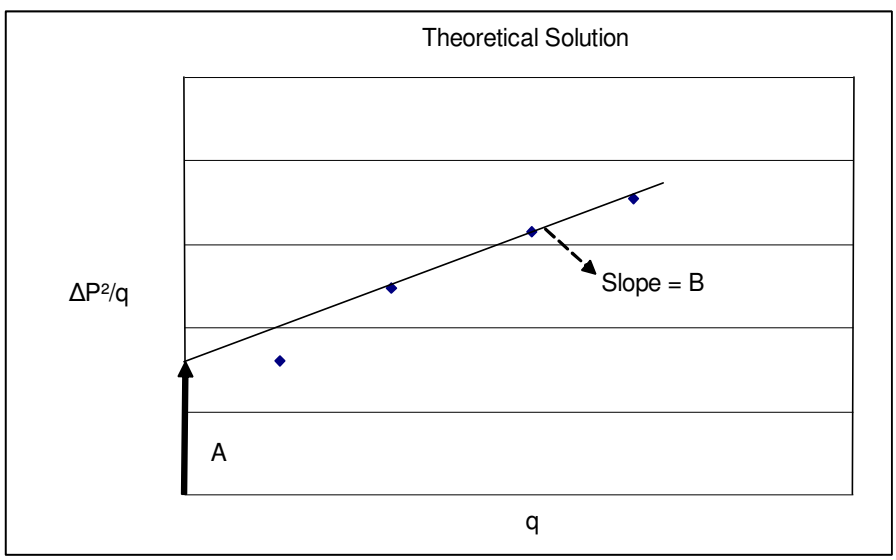

Figure 2.4: Analysis of Data-Houpeurt method for flow after flow test

Once coefficients *A* and *B* are calculated, they can be plugged into the Equation (21) to determine the well's deliverability.

2.8.2 Pressure-Transient Tests Analysis

Drawdown test analysis

In order to analyze drawdown test, the following procedure must be followed:

Prepare a plot of ΔP^2 vs. time on log-log paper

- Draw the unit-slope line through early part of data
- Determine end of unit-slope line, t^*
- Multiply t^* by 50 to calculate end of wellbore storage, t_{wbs}

Prepare a plot of P^2 vs. time on semi-log paper

- Draw the best straight line starting at t > t_{wbs}
- Obtain the slope (m)
- If the straight line has a positive slope, the well is an injection well and if the straight line has a negative slope, the well is a production well.

Calculate *k* using:

$$k = \frac{1637 q T \overline{\mu z}}{mh} \tag{35}$$

Calculate *S'* using:

$$S' = 1.151\left[\frac{P_{1hr}^2 - P_{wf}^2}{m} - \log\left(\frac{k}{\phi \overline{\mu c} r_w^2}\right) + 3.23\right] \tag{36}$$

$S' = s + Dq_1$ Drawdown test 1

$S' = s + Dq_n$ Drawdown test *n*

Now that *k*, *s* and *D* are determined, deliverability equation for the well can be determined using Equation (21), (23) and (24).

Sometimes during the pressure-transient tests, the flow rate is not constant. In order to analyze these types of test, following procedure must be followed:

Log-log plot of $\frac{\Delta P^2}{q}$ vs. time

- Draw the unit-slope line
- Determine t^*, multiply t^* by 50 to calculate t_{wbs}

Semi-log plot of $\frac{\Delta P^2}{q}$ vs. time

- Draw the best straight line starting through the points
- Obtain the slope (m)

Calculate *k* using:

$$k = \frac{1637T\overline{\mu z}}{mh} \tag{37}$$

Calculate *S'* using:

$$S' = 1.151\left[\left(\frac{P_{1hr}^2 - P_{wf}^2}{q}\right)\times\frac{1}{m} - \log\left(\frac{k}{\phi\overline{\mu c}r_w^2}\right) + 3.23\right] \tag{38}$$

S' = s + Dq_1 Drawdown test 1

S' = s + Dq_n Drawdown test *n*

Falloff test analysis

Log-log plot of ΔP^2 vs. time

- Draw the unit-slope line
- Determine t^*, multiply t^* by 50 to calculate t_{wbs}

Semi-log plot of P^2_{ws} vs. Horner time ($\frac{t_p + \Delta t}{\Delta t}$)

- Draw the best straight line starting through the points
- Obtain the slope (m)

Calculate *k* using equation (20)

Calculate *S'* using:

$$S' = 1.151\left[\frac{P^2_{wf} - P^2_{1hr}}{m} - \log\left(\frac{k}{\phi\overline{\mu c} r_w^2}\right) + 3.23\right] \tag{39}$$

CHAPTER 3

OBJECTIVE AND METHODOLOGY

3.1 Description

The goal of this study was to develop reservoir-specific β correlation and to introduce a simple and reliable method to determine gas well deliverability. To achieve the objective, a methodology consisting of the following 4 steps was employed:

Well Test Data Collection and Analysis

- Well test data from two storage field in Appalachian basin were obtained for the study. They are referred to as reservoir *A* and *B* here.
- Drawdown test analysis was used for test interpretation (analysis) throughout this study. Since reservoirs pressures were less than 1500 psia, pressure-square method was used. For reservoir *B*, there were some falloff tests data available as well, that they were analyzed to verify formation permeability.

Evaluate the Existing β Correlations

- All β correlations were used to determine s using porosity and permeability from single-rate well tests.
- True skin factor was determined for each well using the results of multi-rate drawdown test analysis.
- Comparison of skin factors from two different methods was made.

Propose a methodology to predict deliverability

Develop and verify Reservoir-Specific β Correlation

3.2 Well Test Data Collection and Analysis

Most of the time, for gas storage reservoirs, there is some previous test data available, but for producing reservoirs, there is usually limited data available. In this study the well test data for two storage reservoirs were available. For confidentiality purposes the two reservoirs are referred as reservoir *A* and *B*.

3.2.1 Reservoir *A* Description

Multi-rate tests data are available for 5 wells in reservoir *A*. Reservoir *A* is part of Clinton sand. The Clinton sand is composed of sandstones, shales and interbedded limestone. The color of the Clinton is gray to reddish and the thickness may be as much as 85 feet. To the south this formation is more calcareous; crinoid stems are abundant and there is much resemblance to marble in some localities. The sand from which production is greatest is near the bottom of the group and some geologist consider it a part of the Medina. At several places, stray sands are found just above the Clinton, and are often reported as "red rock." Perhaps this is the bed which thickens to the east and becomes iron ore. To the westward the Clinton thins out and is a shale just beyond the center of Ohio. Here is a fine-grained deposit which requires that the well be shot in order to obtain any production. In the southern part of Ohio, the Clinton is not a good reservoir and contains more limestone; the sand is more porous in central Ohio and is consequently more productive. Table 3.1 summarizes the parameters for reservoir *A*.

Table 3.1: Parameters used for reservoir *A*

Average Formation Porosity, ϕ (%)	14
Pay Zone Thickness, h (ft)	10
Surface Temperature, T_s (°F)	55
Bottomhole Temperature, T_f (ºF)	75
Gas Specific Gravity, γ_g	0.585
Well-bore radius, r_w (ft)	0.3

The wells in reservoir *A* were tested prior to withdrawal cycle and drawdown tests were conducted. The well test data are given in Appendix A.

3.2.2 Reservoir *B* Description

Multi-rate tests data are available for 3 wells in reservoir *B*. Reservoir *B* is located in Harrison County, West Virginia and was discovered in 1931. Storage operations began in 1937. The storage zone is the Upper Devonian Gantz and 50 Feet sands. The structure runs along the Northwest flank of the Southwest plunging Chestnut Ridge Anticline with a trapping mechanism related to a permeability pinchout. The structural relief is 350 feet to 1900 feet deep. The reservoir area is approximately 2895 acres with a total of 36 input/output wells. The sand has been identified as fairly homogeneous with individual samples showing sand grains that have both pebbly and fine textures. The net pay averages less than 50 feet. The average porosity for the sand is less than 15% and the permeability of the sand ranges form 100 mD to 1000 mD that have been confirmed with well testing and core analysis. The discovery pressure for the storage pool was approximately 500 psia. Table 3.2 summarizes the parameters for reservoir *B*.

Table 3.2: Parameters used for reservoir *B*

Average Formation Porosity, ϕ (%)	15
Pay Zone Thickness, h (ft)	40-50
Bottomhole Temperature, T_f (ºF)	75-79
Gas Specific Gravity, γ_g	0.58
Well-bore radius, r_w (ft)	0.167, 0.204, 0.269
Reservoir Depth (ft)	1600-1900
Reservoir Area (acres)	2895

The wells in reservoir *B* were tested at the injection cycle and drawdown and falloff tests were conducted. The well test data are given in Appendix A.

3.2.3 Multi-Rate Test Analysis

In this study, two cases are reviewed for gas well deliverability determination:

Case 1) if multi-rate test data is available

If deliverability test data is available, Houpeurt method analysis must be used in order to determine the well deliverability equation. See section 2.6.1 for the test analysis procedure.

If transient test data is available, transient test analysis must be used, and the results from test analysis must be plugged into Equations (21), (23) and (24) to determine the well deliverability equation. Since drawdown and falloff tests data were used throughout this study, only these two tests analysis procedure were reviewed in this study. See section 2.6.2 for drawdown and falloff test analysis.

Case 2) if only single-test data is available.

First the single-rate test must be analyzed to determine permeability, *k*, and apparent skin factor, *S'*. Using Equation (19), *k* and *S'*, *D* can be calculated if the value of β is known. Use one of the correlations that are developed for β experimentally introduced in section 2.2. Use Equation (18) to calculate true skin factor, *s*. Now that *k*, *D* and *s* are determined, Equations (21), (23) and (24) must be used to determine the well deliverability equation.

3.3 Evaluation of the Existing β Correlations

All single-rate tests were first analyzed, and then the permeability and apparent skin factor were obtained for all flow rates for each well. β correlations introduced in section 2.2 then were evaluated using these permeability and average reservoir porosity, and then *D* was determined using Equation (19). Additionally, true skin factors obtained from test analysis, s_{test} were compared with true skin factors, $s_{equation}$ obtained from Equation (18).

3.3.1 Evaluation of the Existing β Correlations for Wells in Reservoir *A*

A sample evaluation for well 3946 is presented in this section. First permeability and apparent skin factor were obtained for flow rate of 1363.1 Mscf. Then β was evaluated for every single correlation introduced in section 2.2. Once the values for β were determined, *D* was calculated using Equation (19) for each well, and moreover true skin factor, $s_{equation}$, was determined using Equation (18) for every well. Using drawdown

analysis introduced in section 2.6.2, true skin factor, s_{test}, was determined for every well.

When $s_{equation}$ and s_{test} were determined, a simple comparison was made. Table 3.3 summarizes the results of β correlations evaluation for well 3946.

Table 3.3: β correlations evaluation for well 3946 and flow rate 1363.1 Mscf

Q = 1363.1 Mscf	β	$s_{equation}$	s_{test}	Error %
Geertsma	4.950E+07	-2.62	-3.6	27.83
Thauvin & Mohant	5.398E+06	-2.57	-3.6	29.29
Janicek & Katz	4.477E+08	-3.10	-3.6	14.58
Jones	4.749E+08	-3.13	-3.6	13.67
Jones	4.238E+08	-3.07	-3.6	15.37
Coles & Hartman	1.057E+09	-3.84	-3.6	-5.70
Coles & Hartman	2.762E+08	-2.89	-3.6	20.28

3.3.2 Evaluation of the existing β correlations for wells in reservoir *B*

Same procedure that was used for reservoir *A*, was applied for reservoir *B*. In this sample, well 7772 and flow rate of 2750 Mscf were selected. Table 3.4 summarizes the results of β correlations evaluation for well 7772.

Table 3.4: β correlations evaluation for well 7772 and flow rate 2750 Mscf

Q = 2750 Mscf	β	$s_{equation}$	s_{test}	Error %
Geertsma	7.552E+06	-0.21	-1.6	86.54
Thauvin & Mohant	1.085E+06	-0.09	-1.6	94.46
Janicek & Katz	9.983E+06	-0.26	-1.6	83.56
Jones	5.556E+06	-0.18	-1.6	88.98
Jones	4.045E+06	-0.15	-1.6	90.83
Coles & Hartman	3.865E+06	-0.14	-1.6	91.05
Coles & Hartman	1.331E+06	-0.09	-1.6	94.16
Svec & Engler	4.790E+06	-0.16	-1.6	89.92
Pascal et al	1.005E+09	-19.63	-1.6	-1134.57
Tek et al	1.348E+07	-0.33	-1.6	79.28

3.4 Proposed Methodology to Predict Gas Well Deliverability

In order to develop the new method to predict gas well deliverability, previous well tests data are needed. Once the well tests data are available, the following steps must be executed to determine gas well deliverability:

1. Analyze all multi-rate tests and determine k and S' for each flow rate for every well.
2. Using linear regression and Equation (18), calculate D and s.
3. By rearranging Equation (19) and using value of D obtained from step 2, calculate β for every individual well.
4. Take natural logarithm from k and β for every well, plot them on the Cartesian paper, and use linear regression to develop a general correlation for β for corresponding reservoir. Other simple way to do this is to use LOGEST() function in Microsoft Excel and develop the β correlation.

5. Now that the β correlation for specific reservoir is determined, this correlation can be used throughout reservoir life. In order to obtain the true well deliverability in future, one single rate test will be needed for each well. Having one single rate test data, the following steps must be taken to determine well deliverability:
    - Analyze the test and determine k and S'.
    - Calculate D using k from above step and Equation (19).
    - Plug the values of D, S, q and k into Equation (18) and calculate s.
    - Determine the coefficients A and B in Equation (21) using k, D, s and Equations (23) and (24).
    - Determine the well true deliverability using coefficients A and B and Equation (21).

3.5 Developing Reservoir-Specific β Correlation and Verification

3.5.1 Reservoir *A*

Drawdown test data was available for five wells. First a β correlation was developed using wells 3946, 3827, 3931 and 3870, and well 3585 was left out to verify the β correlation we developed with only four wells. Once the verification was confirmed and the accuracy of developed β Correlation was determined, a general β correlation was developed for reservoir A using five wells. For consistency with other β correlations presented in section 2.2, the β correlation was developed in the logarithmic form.

Figure 3.1 illustrates log-log plot of k vs. β to determine β correlation for reservoir A

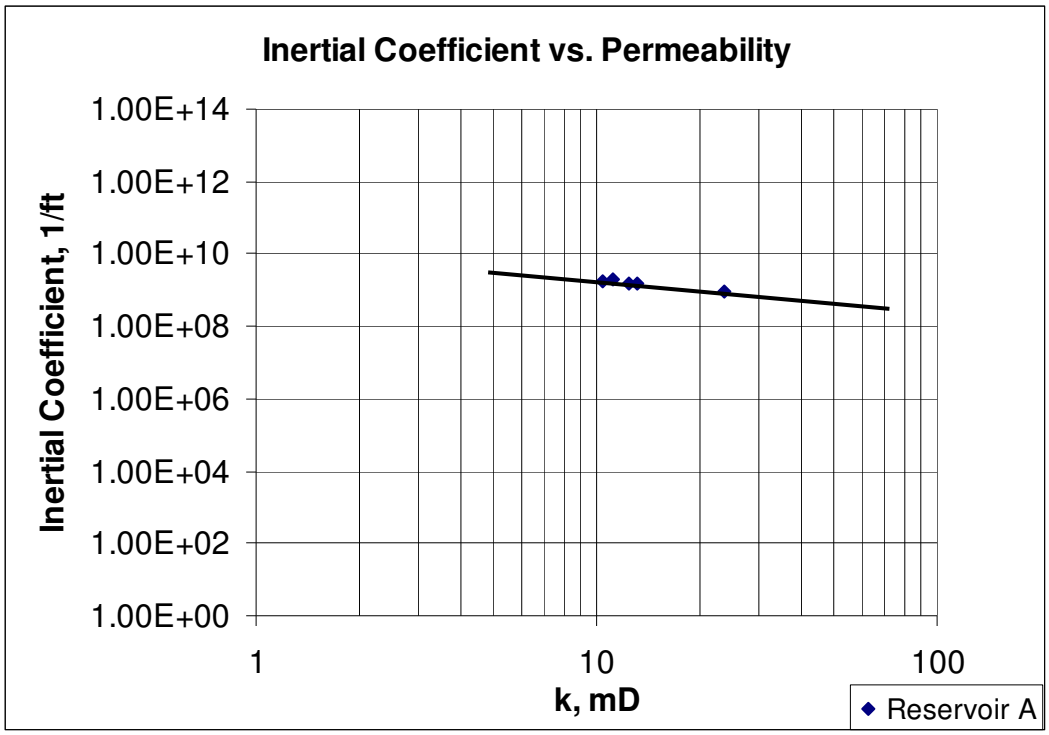

Figure 3.1: Log-log plot of permeability vs. inertial coefficient for reservoir *A* using five wells.

3.5.2 Reservoir *B*

Drawdown test data was available for three wells. The same procedure that was used for reservoir *A*, was applied for reservoir *B*.

CHAPTER 4

RESULTS AND DISCUSSION

The main objective of this study was to develop and evaluate a reliable method for predicting the gas well deliverability without the need for costly and time-consuming multi-rate tests. To do this, first multi-rate tests were analyzed and *k*, *S'*, *D* and *β* were determined for every well. Table 4.1 summarizes drawdown test analysis results for wells in reservoir *A*.

Table 4.1: Drawdown test analysis results for wells in reservoir *A*

Well	k, mD	s	D	β, 1/ft
3585	12.52	-3.05	5.85×10^{-4}	1.61×10^{9}
3946	23.62	-3.63	7.82×10^{-4}	9.28×10^{8}
3827	11.19	-2.31	7.51×10^{-4}	1.87×10^{9}
3931	13.11	-2.97	6.80×10^{-4}	1.48×10^{9}
3870	10.47	-2.32	6.17×10^{-4}	1.72×10^{9}

Table 4.2 summarizes drawdown test analysis results for wells in reservoir *B*.

Table 4.2: Drawdown test analysis results for wells in reservoir *B*

Well	k, mD	s	D	β, 1/ft
9096	5.77	-2.456	5.00×10^{-4}	1.01×10^{10}
7772	527.74	-1.59	7.20×10^{-4}	9.71×10^{7}
6065	30.55	-3.25	5.82×10^{-4}	1.69×10^{9}

Existing β Correlations Evaluation:

The β correlations developed experimentally are presented in section 2.2. They were evaluated using permeability obtained from well test analysis results, and then D was determined using equation (19). True skin factor, $s_{equation}$, was calculated using equation (18) for every well. True skin factor, s_{test}, also was calculated from well tests analysis. At the end, $s_{equation}$ was compared with s_{test} for every well to determine the errors that using experimental β correlations could generate. Table 4.3 summarizes the results for well 3946 and flow rate of 2002.64 Mscf located in reservoir *A*.

Table 4.3: β correlations evaluation for well 3946 and flow rate 2002.64 Mscf

Q = 2002.64 Mscf	β	$s_{equation}$	s_{test}	Error %
Geertsma	5.207E+07	-2.14	-3.6	40.94
Thauvin & Mohant	5.679E+06	-2.07	-3.6	43.00
Janicek & Katz	5.081E+08	-2.88	-3.6	20.72
Jones	5.512E+08	-2.95	-3.6	18.81
Jones	4.959E+08	-2.86	-3.6	21.26
Coles & Hartman	1.279E+09	-4.12	-3.6	-13.45
Coles & Hartman	3.312E+08	-2.59	-3.6	28.57
Svec & Engler	1.142E+08	-2.24	-3.6	38.19
Pascal et al	3.861E+10	-64.20	-3.6	-1668.48
Tek et al	5.579E+08	-2.96	-3.6	18.51

Table 4.4 summarizes the results for well 7772 and flow rate of 5203 Mscf located in reservoir *B*.

Table 4.4: β correlations evaluation for well 7772 and flow rate 5203 Mscf

Q = 5203 Mscf	β	$s_{equation}$	s_{test}	Error %
Geertsma	7.472E+06	1.49	-1.6	193.67
Thauvin & Mohant	1.074E+06	1.73	-1.6	208.78
Janicek & Katz	9.718E+06	1.40	-1.6	188.37
Jones	5.383E+06	1.57	-1.6	198.61
Jones	3.913E+06	1.62	-1.6	202.08
Coles & Hartman	3.712E+06	1.63	-1.6	202.55
Coles & Hartman	1.281E+06	1.72	-1.6	208.30
Svec & Engler	4.688E+06	1.59	-1.6	200.25
Pascal et al	9.799E+08	-35.03	-1.6	-2103.068
Tek et al	1.314E+07	1.28	-1.6	180.29

Develop and Verify β Correlation for Reservoir *A* and *B*:

1) Reservoir *A*

The inertial coefficient for every well was determined using well tests analysis. To develop a β correlation for reservoir *A* and reservoir *B*, a plot of β versus *k* (from Table 4.1) on log-log paper was prepared.

Wells 3946, 3827, 3931 and 3870 were used to develop β correlation for reservoir *A,* well 3585 was left out for verification purposes. Once β correlation was developed with only four wells, and it was verified using well 3585 formation permeability, the final β correlation for reservoir *A* was developed using five wells.

Figure 4.1 illustrates a plot of *k* vs. β on the log-log paper using 4 wells for reservoir *A*.

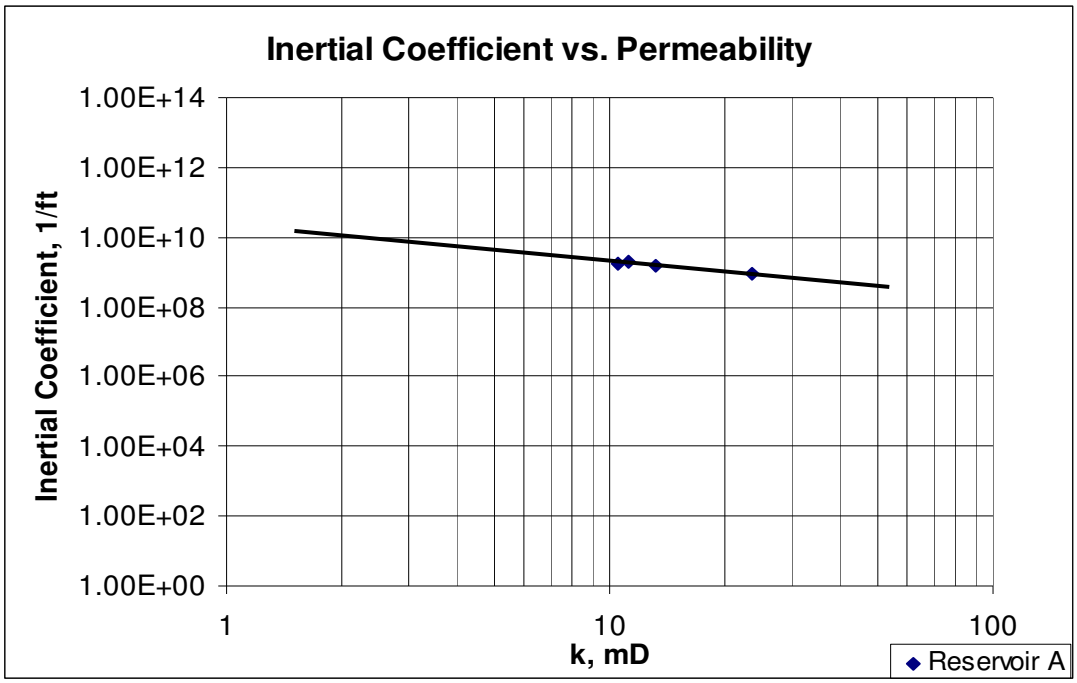

Figure 4.1: Log-log plot of permeability versus inertial coefficient for reservoir *A* using only 4 wells.

Using four wells, the β correlation was as follows:

$$\beta = \frac{1\times10^{10.11}}{k^{0.83}} \qquad (40)$$

To verify whether the correlation was reliable or not, the permeability of well 3585 was plugged into Equation (40) and β value was determined. The value of β obtained from drawdown tests, and the value of β obtained from Equation (40), was then compared.

The value of β from drawdown tests for well 3585 was 1.61×10^{9} 1/ft, and the value of β from Equation (40) was 1.5×10^{9} 1/ft. By comparing these two numbers, Equation (40) generated only 2 % error. The small percentage of error indicated that Equation (40) was reliable and accurate. After verifying Equation (40), five wells were used to develop the final β correlation for reservoir *A*.

Figure 4.2 illustrates plot of *k* vs. β on the log-log paper using 5 wells for reservoir *A*.

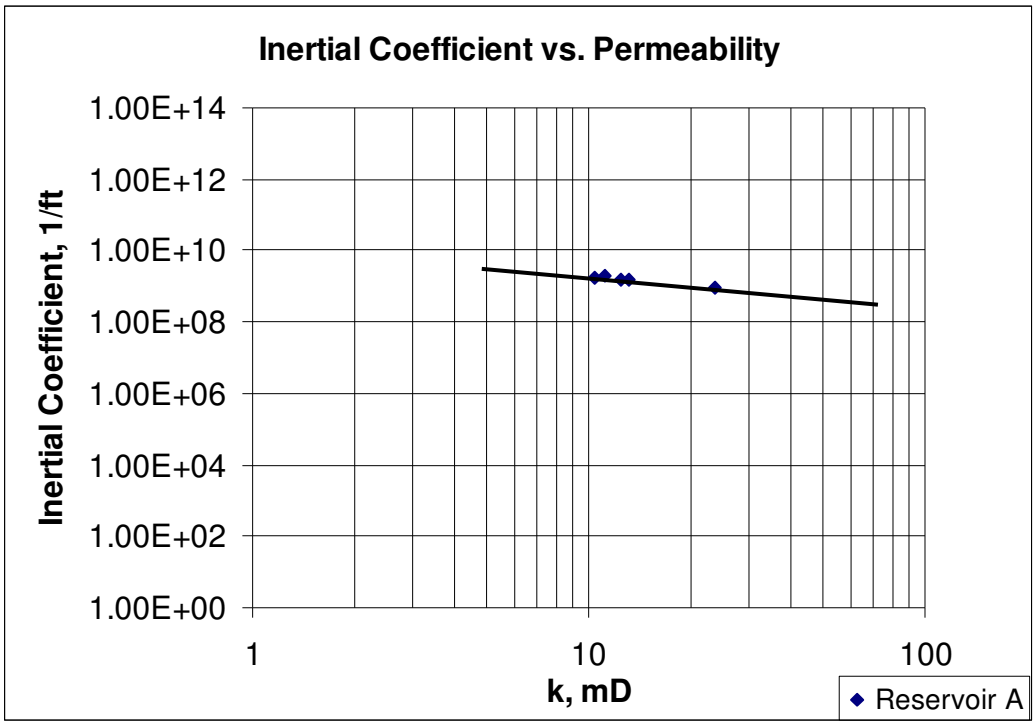

Figure 4.2: Log-log plot of permeability vs. inertial coefficient for reservoir *A* using only 5 wells.

After using β values from five wells, and plotting them versus permeability on the log-log paper, the final β correlation for reservoir *A* was as follows:

$$\beta = \frac{1\times 10^{10.115}}{k^{0.835}} \qquad (41)$$

Table 4.5 summarizes the comparison between β calculated from Equation (41) and β obtained from drawdown tests analysis for reservoir *A*.

Table 4.5: Comparison of β from 2 methods

Well	β, 1/ft (Test)	β, 1/ft (Equation 41)	Error (%)
3946	9.33E+08	9.29E+08	0.4
3827	1.87E+09	1.78E+09	5.0
3931	1.48E+09	1.51E+09	2.1
3870	1.72E+09	1.82E+09	5.7
3585	1.61E+09	1.57E+09	2.3

True skin factor was calculated using Equations (41), (19) and (18), and drawdown test analysis results; a simple comparison next was made. To calculate *s* using Equation (41), first β was obtained using Equation (41), then the value of β was plugged into Equation (19) and *D* was obtained. Once *D* was determined, it was plugged into Equation (18) and *s* was calculated. Table 4.6 summarizes the results of comparison of *s* from 2 methods for reservoir *A*.

Table 4.6: Comparison of *s* from 2 methods, reservoir *A*

Well	q (Mscf)	s (Test)	s (Equation)	Error (%)
3946	1363.1	-3.63	-3.63	0
	2002.64	-3.63	-3.61	0.5
3585	1301.34	-3.05	-3.045	0.15
	2320.43	-3.05	-3.28	7.5
3827	308.32	-2.31	-2.4	4
	670.26	-2.31	-2.11	8
	1171	-2.31	-2.34	1.3
3931	820.19	-2.97	-3.05	2.6
	1381.4	-2.97	-2.9	2.5
	2082.39	-2.97	-3.03	2.1
3870	942.43	-2.23	-2.25	1.2
	1639.57	-2.23	-2.31	3.8

2) Reservoir *B*

Similar procedure was used to develop β correlation for reservoir *B* using 6065, 7772 and 9096 wells. Permeability was plotted versus β (from Table 4.2) on a log-log paper and β correlation was developed for reservoir B. Figure 4.3 illustrates a plot of *k* vs. β on the log-log paper using 3 wells for reservoir *B*.

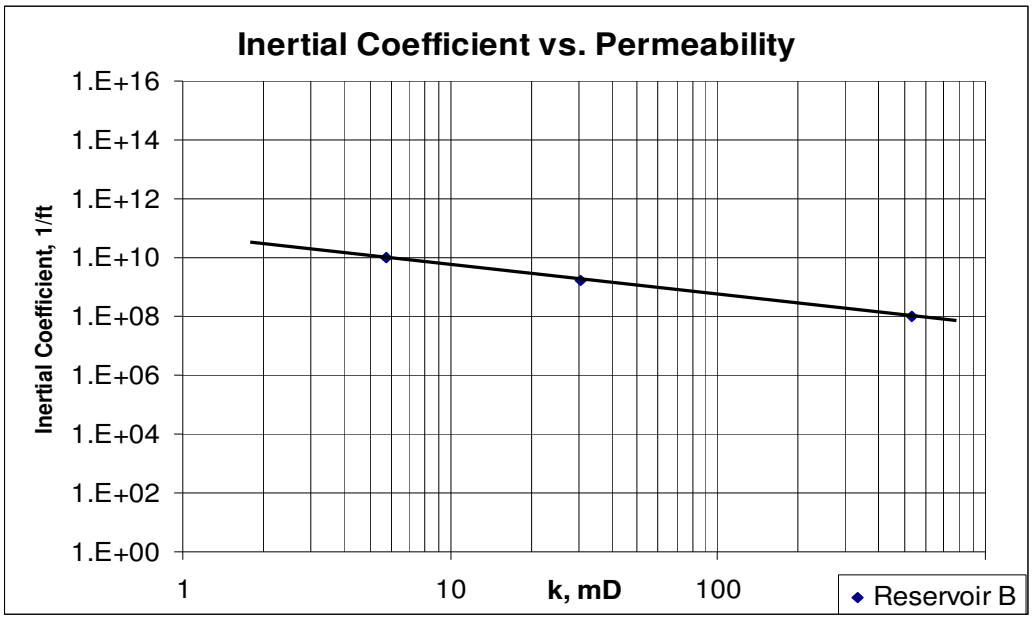

Figure 4.3: Log-log plot of permeability vs. inertial coefficient for reservoir *B* using 3 wells.

After using β values from three wells, and plotting them versus permeability on the log-log paper, the final β correlation for reservoir *B* was as follows:

$$\beta = \frac{1\times10^{10.79}}{k^{1.029}} \qquad (42)$$

Table 4.7 summarizes the comparison between β calculated from Equation (42) and β obtained from drawdown tests analysis for reservoir *B*.

Table 4.7: Comparison of β from 2 methods

Well	β, 1/ft (Test)	β, 1/ft (Equation 42)	Error (%)
9096	1.012×10^{10}	1.01×10^{10}	0.0
7772	9.71×10^{7}	9.71×10^{7}	0.0
6065	1.685×10^{9}	1.76×10^{9}	4.0

Table 4.8 summarizes the results of comparison of *s* from 2 methods for reservoir *B*.

Table 4.8: Comparison of *s* from 2 methods, reservoir *B*

Well	q (Mscf)	s (Test)	s (Equation)	Error (%)
9096	350	-2.465	-2.35	4.8
	430	-2.465	-2.31	5.8
6065	1450	-3.25	-2.98	8
	1749	-3.25	-3.01	7.3
	2302	-3.25	-2.99	8
7772	2750	-1.59	-1.51	4
	5203	-1.59	-1.43	9

Equation (5) generates the lowest errors for both reservoirs. Table 4.9 summarizes the results of β comparison from drawdown test and Equation (5).

Table 4.9: Comparison of β from test and Equation (5)

K (mD)	β (test)	β (Equation 5)	Error (%)
23.615	9.28E+08	524240273	43
11.19	1.87E+09	1.285E+09	31
13.11	1.48 E+09	1.062E+09	28
10.47	1.72 E+09	1.391E+09	19
12.52	1.61 E+09	1.123E+09	30
5.77	1.01 E+10	2.844E+09	71
527.74	9.7 E+07	1.26 E+07	87
30.55	1.69 E+09	3.84 E+08	77

CHAPTER 5

CONCLUSIONS AND RECOMMENDATIONS

In this study, a simple and reliable method to determine gas well deliverability was developed. From this study the following conclusions have been made:

1) Reservoir-specific β correlation was developed based on the previous well tests data, and a new method to determine gas well deliverability using reservoir-specific β correlation was introduced.

2) The new method was applicable when single-rate test data was available; therefore eliminating multi-rate tests that were cumbersome and time-consuming.

3) Using data from one single-rate test and reservoir-specific β correlation, one can determine the true skin factor, the non-Darcy coefficient, the deliverability equation coefficients A and B, and the true deliverability equation for every individual well in the corresponding reservoir.

4) True skin factor for each well was calculated using ten β correlations that were introduced in section 2.2, the significant error these β correlations generated while determining true skin factor was also investigated.

5) In this study, the reservoirs were composed of sandstone and limestone. Some of the experimental β correlations that were defined for sandstone and limestone reservoirs did not generate the same true skin factor as the well tests analysis. It can be concluded that since each reservoir has its own specific characterization, no two reservoirs will be identical, even if they have the same composition.

6) The reservoirs in this study were part of the same field (Appalachian basin), but the β correlations developed for these reservoirs were not the same. It can be concluded that one β correlation can not be used for the entire field and β correlation must be developed for every reservoir.

RECOMMENDATION

If reservoir permeability varies in a wide range, it is recommended to obtain data from wells that represent various permeability to develop β correlation with more accuracy.

Reservoir *A* and *B* are part of the same field, but the β correlations developed for these reservoirs were different. I recommend an in-depth study to be conducted to investigate the impact of the other characteristics of reservoir on inertial coefficient beside permeability and porosity.

If there were no multi-rate test data available for reservoir *A* and *B*, I would recommend one could use Tek et al. correlation (Equation 5) to evaluate inertial coefficient.

REFRENCES

Firoozabadi, A. and Katz, D.L.: "An Analysis of High-Velocity Gas Flow through Porous Media" JPT (Feb. 1979), 211-216

H.A. Belhaj, K.R. Agha, A.M. Nouri, S.D. Butt, H.F. Vaziri, M.R. Islam, Dalhousie University, "Numerical Simulation of Non-Darcy Flow Utilizing the New Forchheimer's Diffusivity Equation" SPE 81499-MS, Middle East Oil Show, 9-12 June 2003, Bahrain.

Milton-Tayler, D.: "Non-Darcy Gas Flow: From Laboratory Data to Field Prediction" SPE 26146, presented at the Gas Technology Symposium, Calgary, Alberta, Canada, June 28-30, 1993

J.P. S;pivey, SPE, K.G. Brown, SPE, W.K. Sawyer, SPE, and J.H. Frantz, SPE, Schlumberger, "Estimating Non-Darcy coefficient from Buildup Test with Wellbore Storage" SPE 77484, presented at the SPE Annual Technical Conference and Exhibition held in San Antonio, Texas, 29 September – 2 October 2002.

Civan, F., and Evans, R.D.: "Determination of Non-Darcy Flow Parameters Using a Differential Formulation of the Forchheimer Equation," SPE 35621 presented at the 1996 SPE Gas Technology Conference, Calgary, Alberta, Canada, April 28 – May 1.

Barree, R.D. and Conway, M. W.: "Beyond Beta Factors: A Complete Model for Darcy, Forchheimer, and Trans-Forchheimer Flow in Porous Media" SPE 89325, presented at the SPE annual Technical Conference and Exhibition, Houston, TX, Sept. 26-59, 2004

A.W. Brannon, CNG Transmission Crop., K. Aminian, S. Ameri, and H.I. Bilgesu, West Virginia University, "A New Approach for Testing Gas Storage Wells" SPE 39223, presented at the 1997 SPE Eastern Regional Meeting held in Lexington, KY, 22-24 October 1997.

Barak, A.Z.: "Comments on High-Velocity Flow in Porous Media" by Hassanizadeh and Gary," Transport in Porous Media (1987) 1, 63-97.

Ma, H., and Ruth, D.W.: "Physical Explanations of Non-Darcy Effects for Fluid Flow in Porous Media," SPE 26150 presented at the 1993 SPE Gas Technology, Calgary, Canada, June 28-30.

Alvarez, C., Holditch, S., and McVay, D., "Effects of Non-Darcy Flow on Pressure Transient Analysis of Hydraulically Fractured Gas Wells" SPE 77468-MS, presented at 2000 Annual Technical Conference and Exhibition, San Antonio, Texas, USA, 29 September 29 – October 2, 2000.

Chase, R.W., Alkandari, H., "Prediction of Gas Well Deliverability from a Pressure Buildup or Drawdown Test" SPE 26915, presented at 1993 SPE regional conference, PA, WV, USA, 2-4 November 1993.

Cornell, D. and Katz, D.L.: "Flow of Gases through Consolidated Porous Media," Industrial and Engineering Chemistry (Oct. 1953) 45, 2145.

Narayanaswamy, G., Sharma, M.M., and Pope, G.A.: “Effect of Heterogeneity on the Non-Darcy Flow Coefficient,” SPE Reservoir Eval. & Eng. (June 1999) 296-302.

Dacun, L., “Analytical Study of the Wafer Non-Darcy Flow Experiments,” SPE 76778, presented at 2000 Western Regional/AAPG Pacific Section Joint Meeting, Anchorage, Alaska, May, 20-22, 2000.

Kutasov, I.M.: “Equation Predicts Non-Darcy Flow Coefficient,” Oil & Gas Journal (March 15, 1993) 66-67.

Forchheimer, P.: "Wasserbewewegung durch Boden," ZVDI (1901) 45, 1781.

Geertsma, J.: "Estimating the Coefficient of Inertial Resistance in Fluid Flow through Porous Media," SPE 4706, SPE J. (Oct. 1974) 445-450.

Guppy, K. H., Cinco-Ley, H., Ramey, Jr. H. J., and Sameniego V., F.: “Non-Darcy Flow in Wells with Finite-Conductivity Vertical Fractures” SPEJ (Oct. 1982) 681

Katz, D. L., Cornell, D., Kobayashi, R., Poettmann, F. H., Vary, J. A., Elenbaas, J. R. and Weinaug, C. F.: Handbook of Natural Gas Engineering, McGraw-Hill Book Co. Inc., New York, 1959.

Li, Dacun., Englar, TW, “Literature Review on Correlations of Non-Darcy Coefficient” SPE 70015, presented at SPE Permian Basin Oil and Gas Recovery conference, Midland, Texas, USA, 15-16 May 2001.

Li, D., Svec, R.K., Engler, T.W., and Grigg, R.B.: “Modeling and Simulation of the Wafer Non-Darcy Flow Experiments,” paper SPE 68822, Proc., the 2001 SPE Western Regional Meeting, Bakersfield, CA, March 26-30.

SLB, I. Schlumberger Oilfield Glossary, Available: http://www.slb.com

Tek, M.R., Coats, K.H., and Katz, D.L.: "The Effect of Turbulence on Flow of Natural Gas through Porous Media," SPE 147, JPT, July 1962

Thauvin, F., and Mohanty, K.K.: "Network Modeling of Non-Darcy Flow through Porous Media," Transport in Porous Media (1998) 31, 19-37.

Umnuayponwiwat, S., Ozkan, E., Pearson, C. and Vincent, M., “Effect of non-Darcy Flow on the Interpretation of Transient Pressure Responses of Hydraulically Fractured Wells,” SPE 63176, presented at the 2000 SPE Annual Technical Conference and Exhibition, Dallas, Texas, U.S.A, October 1-4, 2000.

Lee, W.J.: Well Testing, SPE Textbook Series, Richardson, TX (1982).

F. Thauvin and K. K. Mohanty, University of Houston, “Modeling of Non-Darcy Flow through Porous Media” SPE 38017, presented at the 1997 SPE Reservoir Simulation System held in Dallas, Texas, 8-11 June, 1997.

S.C. Jones, Core Research. Div. of Western Atlas, "Using the inertial Coefficient, β, To Characterize Heterogeneity in Reservoir Rock" SPE 16949, presented at the 62nd Annual Technical Conference and Exhibition of the SPE held in Dallas, Texas September 27-30 1987.

Cornell, D. and Katz, D.L.: "Flow of Gases through Consolidated Porous Media" Industrial and Engineering Chemistry (Oct. 1953) 45, 2145

Liu, X., Civan, F., and Evans, R.D.: "Correlation of the Non-Darcy Flow Coefficient," J. Cdn. Pet. Tech. (Dec. 1995) 34, No. 10, 50-54.

Gewers, C.W.W. and Nichol, L.R.: "Gas Turbulence Factor in Microvugular Carbonate," j.Cdan. Pet Tech.(April-June 1969) 31.

Pascal, H., Quillian, R.G. and Kingston, J.: "Analysis of Vertical Fracture Length and Non-Darcy Flow Coefficient Using Variable Rate Test" SPE 9438, presented at the 1980 SPE Annual Technical Conference and Exhibition, Dallas, September 21-24.

Coles, M.E. and Hartman, K.J.: "Non-Darcy Measurement in Dry Core and the Effect of Immobile Liquid" SPE 39977, presented at the 1998 SPE Gas Technology Symposium, Calgary, Alberta, Canada, March 15-18

Belhaj, H.A., Agha, K.R, Nouri, A.M., Butt, S.D., Isalm, M.R. and Vaziri, H.F.: "Numerical Modeling of Forchheimer's Equation to Describe Darcy and Non-Darcy Flow in Porous Medium System" SPE 80440 proc., the SPE Asia Pacific Oil and Gas Conference and Exhibition, Jakarta, Indonesia, April 15-17, 2003.

R. Norman and J.S. Archer, Imperial college:" The effect of pore structure on non-Darcy gas flow in some low permeability reservoir rocks" SPE/DOE 16400, presented at the SPE/DOE low permeability reservoirs symposium held in Denver, Colorado May 18-19 1987.

APPENDIX A

Reservoir *A* and *B* Well Tests Data

Drawdown Test Data for Wells in Reservoir *A*:

Drawdown test data for wells 3585, 3946, 3827, 3931 and 3870 were available.

Table A.1: Drawdown tests data for well 3585

Δt, Hrs	q = 1301 Mscf	q = 2320 Mscf
	P, psia	P, psia
0	1109.2	1121.7
0.0056	1091.21	1080.65
0.0069	1088.21	1073.54
0.0084	1085.41	1066.81
0.0139	1075.66	1043.09
0.025	1061.29	1006.61
0.0361	1049.8	979.64
0.0417	1047.6	968.84
0.057	1039.6	945.11
0.0709	1033.8	929.34
0.0875	1026.2	912.21
0.1014	1023.1	906.17
0.2736	1006.2	861.31
0.3708	1001.04	849.8
0.4375	997.6	844.12
0.5403	993.6	835.91
0.6306	989.4	829.96
0.7417	987.2	824.1

Table A.2: Drawdown tests data for well 3946

Δt, Hrs	q = 1363 Mscf	q = 2002 Mscf
	P, psia	P, psia
0	881.87	888.82
0.0056	872.45	877.43
0.0069	870.91	874.33
0.0084	869.54	871.65
0.0139	865.45	863.45
0.025	858.21	848.60
0.0361	853.65	839.45
0.0417	850.35	835.24
0.057	845.20	826.85
0.0709	841.45	819.35
0.0875	838.05	812.12
0.1014	834.35	804.52
0.2736	820.24	774.24
0.3708	816.60	767.12
0.4375	815.05	763.46
0.5403	813.14	760.14
0.6306	812.35	757.04
0.7417	811.32	754.44

Table A.3: Drawdown tests data for well 3827

Δt, Hrs	q = 308.32 Mscf	q = 670.26 Mscf	q = 1171.00 Mscf
	P, psia	P, psia	P, psia
0	819.40	809.70	817.30
0.0056	815.53	801.97	804.33
0.0069	814.98	800.40	801.85
0.0084	814.34	798.73	799.30
0.0139	812.24	794.56	791.46
0.025	808.42	786.17	775.14
0.0361	805.31	779.12	762.40
0.0417	804.28	770.26	757.04
0.057	801.12	769.20	743.84
0.0709	799.04	763.34	728.32
0.0875	797.80	757.14	721.08
0.1014	795.16	752.30	713.45
0.2736	784.59	728.46	665.27
0.3708	782.92	724.04	656.98
0.4375	782.30	722.06	654.02
0.5403	781.28	721.12	649.86
0.6306	780.86	720.56	647.92
0.7417	780.54	719.94	645.18

Table A.4: Drawdown tests data for well 3931

Δt, Hrs	q = 820.19 Mscf	q = 1381.40 Mscf	q = 2082.39 Mscf
	P, psia	P, psia	P, psia
0	988.30	988.00	996.29
0.0056	982.65	977.02	977.26
0.0069	981.30	976.08	974.86
0.0084	980.21	972.46	970.00
0.0139	976.08	963.70	957.62
0.025	969.02	949.82	933.94
0.0361	963.14	940.34	916.35
0.0417	961.22	936.45	910.12
0.057	955.90	923.00	892.78
0.0709	952.10	915.62	876.36
0.0875	947.94	906.88	846.42
0.1014	944.88	900.14	812.53
0.2736	931.52	864.42	782.45
0.3708	929.68	858.36	770.31
0.4375	929.01	855.60	765.88
0.5403	928.36	853.02	759.43
0.6306	928.34	850.89	757.18
0.7417	928.33	848.80	756.32

Table A.5: Drawdown tests data for well 3870

Δt, Hrs	q = 942 Mscf	q = 1639 Mscf
	P, psia	P, psia
0	1112.58	1106.40
0.0056	1105.90	1095.40
0.0069	1104.20	1092.50
0.0084	1102.69	1079.70
0.0139	1095.9	1080.34
0.025	1086.03	1062.82
0.0361	1077.24	1048.35
0.0417	1074.35	1042.82
0.057	1064.40	1027.14
0.0709	1057.68	1014.24
0.0875	1050.11	1002.62
0.1014	1042.96	992.55
0.2736	1008.08	930.78
0.3708	1000.84	916.92
0.4375	997.62	911.02
0.5403	993.58	955.00
0.6306	991.25	901.24
0.7417	989.73	899.20

Drawdown and Falloff Tests Data for Wells in Reservoir *B*:

Drawdown and falloff tests data were available for wells 9096, 7772 and 6065.

Table A.6: Drawdown tests data for well 9096

Δt, Hrs	q = 350 Mscf	q = 430 Mscf
	P, psia	P, psia
0	292.6	293.1
0.017	299.3	302.4
0.050	306.6	310.8
0.083	311.8	317.0
0.167	317.6	324.8

Table A.7: Falloff test data for well 9096

Time (hrs)	P_{ws} , psia
0	324.9
0.001383	324.4
0.002783	323.3
0.004167	322.3
0.00555	321.2
0.00695	320.2
0.008333	319.1
0.016667	315
0.033333	309.8
0.05	306.1
0.066667	302.5
0.083333	299.3
0.116667	296.2
0.166667	294.1
0.25	293.1
0.333333	292.6
0.5	292.1

Table A.8: Drawdown tests data for well 7772

Δt, Hrs	q = 2750 Mscf	q = 3400 Mscf	q = 5203 Mscf
	P, psia	P, psia	P, psia
0	290.3	291.3	292.3
0.017	299.3	304.1	316.2
0.050	306.6	305.1	317.2
0.083	311.8	305.8	318.8
0.167	317.6	306.3	319.8

Table A.9: Falloff test data for well 7772

Time (hrs)	P_{ws} , psia
0	331.7
0.001383	315.1
0.002783	306.8
0.004167	303.7
0.00555	302.7
0.00695	302.2
0.008333	300.6
0.016667	299.6
0.033333	298.5
0.05	297.5
0.083333	296.5
0.116667	296
0.166667	295.4
0.5	294.4

Table A.10: Drawdown tests data for well 6065

Δt, Hrs	q = 1450 Mscf	q = 1749 Mscf	q = 2302 Mscf
	P, psia	P, psia	P, psia
0	288.4	289.4	289.9
0.017	305.4	309.4	322.9
0.050	313.7	319.8	336.4
0.083	315.7	324.0	340.5
0.167	319.3	325.0	343.6

Table A.11: Falloff test data for well 6065

Time (hrs)	P_{ws} , psia
0	343.9
0.001383	336.7
0.002783	331.5
0.004167	323.2
0.00555	318
0.00695	315.9
0.008333	313.8
0.016667	307.6
0.033333	303.4
0.05	299.3
0.066667	297.2
0.083333	295.1
0.116667	293.1
0.166667	291.5
0.25	290.5
0.333333	289.4
0.416667	288.9
0.5	288.9

APPENDIX B

MULTI-RATE TEST ANALYSIS AND CALCULATION

Drawdown Test Analysis for Reservoir *A*:

For reservoir *A* one sample calculation is presented. The results of test analysis are tabulated in the following tables:

Well 3585

Table B.1: Gas properties at 75 º F for well 3585

q (Mscf)	$\overline{P}$ (psia)	$\overline{z}$	$\overline{\mu}$ (cp)	$\overline{c}_t$ (psia^{-1})
1301.34	1030.72	0.866	0.0126	0.00077
2320.43	928.16	0.878	0.0123	0.0008484

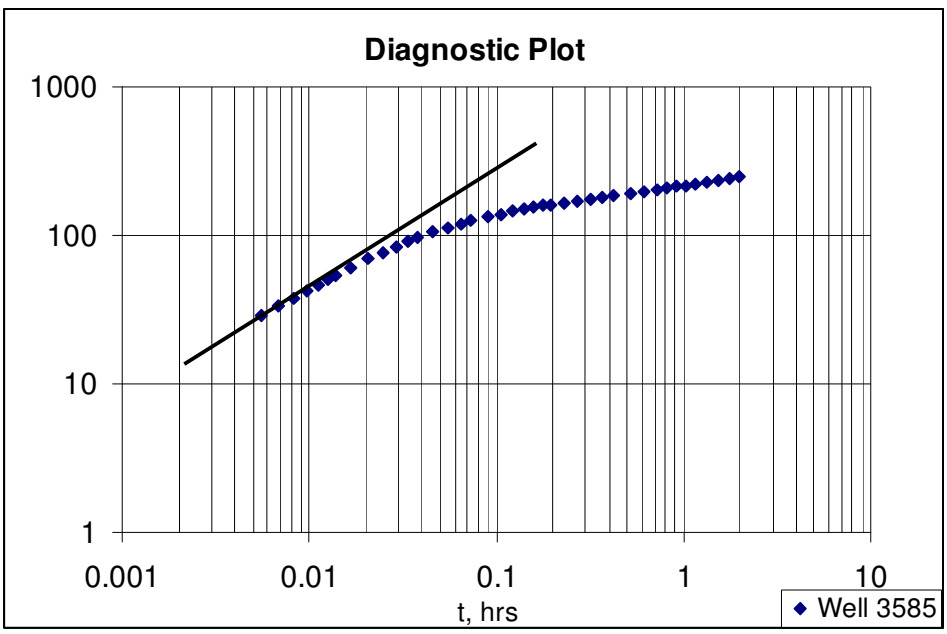

Figure B.1: Drawdown log-log plot for well 3585, q = 1301.34 Mscf

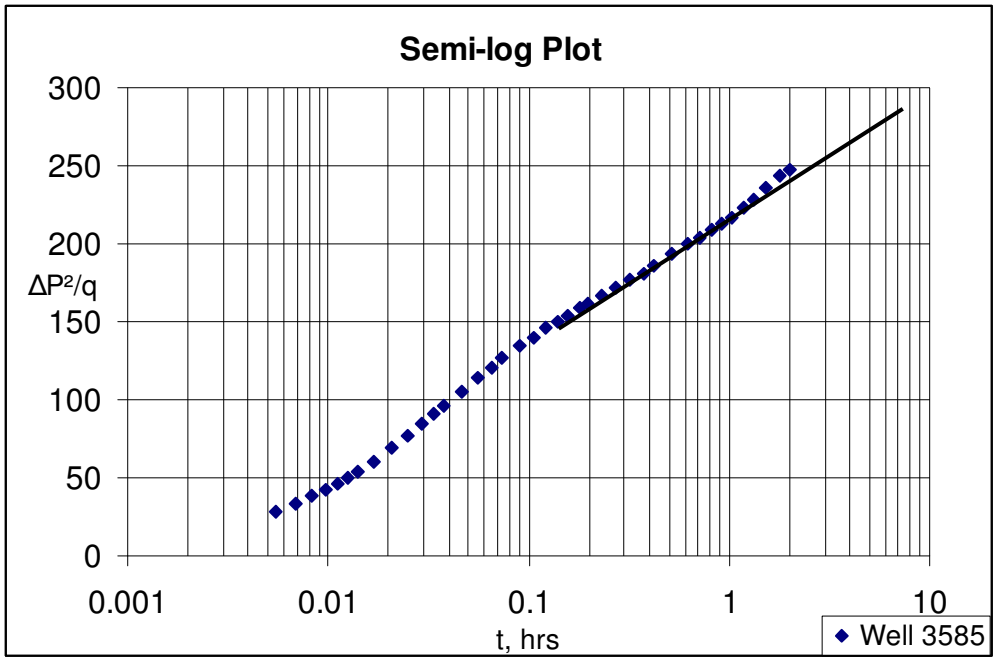

Figure B.2: Drawdown semi-log plot for well 3585, q = 1301.34 Mscf

$$\left(\frac{\Delta P^2}{q}\right)_{1hr} = 213 \text{ psia/Mscf}$$

$$P_{wf} / q = 140 \text{ psia/Mscf}$$

m = 73 psia/q/cycle

$$k = \frac{1637 \times 535 \times 0.0126 \times 0.866}{73 \times 10} = 13.06\ mD$$

$$S' = 1.151\left[\frac{213-140}{73}\right] - \log\left(\frac{13.06}{0.14 \times 0.0126 \times 0.00077 \times 0.3^3}\right) + 3.23 = -2.16$$

Using linear regression: For q = 2320.43 Mscf k = 10.18 and S' = -1.74

D = 6.8×10^{-4}

s = -2.97

Rearranging equation (19):

$$\beta = \frac{6.8 \times 10^{-4} \times 0.01245 \times 10 \times 0.3}{2.22 \times 10^{-15} \times 0.58 \times 12.52} = 1.61 \times 10^{9} \text{ 1/ft}$$

Well 3946

Table B.2: Gas properties at 75 º F for well 3946

q (Mscf)	$\overline{P}$ (psia)	$\overline{z}$	$\overline{\mu}$ (cp)	$\overline{c}_t$ (psia^{-1})
1363.1	841.3	0.88	0.0121	0.0013263
2002.64	888.8	0.882	0.0122	0.0012606

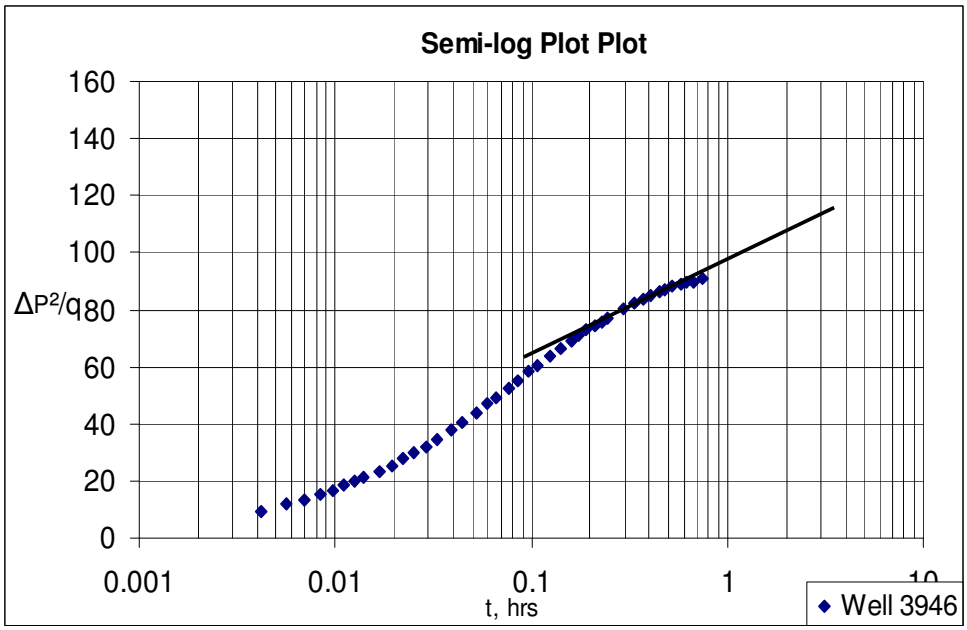

Figure B.3: Drawdown semi-log plot for well 3946, q = 1363.1 Mscf

Table B.3: *k* and *S'* for well 3946

q, Mscf	k, mD	S'
1363.1	24.81	-2.56
2002.64	22.42	-2.06

Table B.4: *D* and *s* for well 3946

D	s	β, 1/ft
7.82×10^{-4}	-3.63	9.3×10^{8}

Well 3827

Table B.5: Gas properties at 75 º F for well 3827

q (Mscf)	$\overline{P}$ (psia)	$\overline{z}$	$\overline{\mu}$ (cp)	$\overline{c}_t$ (psia^{-1})
308.32	798.66	0.893	0.0120	0.00139
670.26	758	0.898	0.0120	0.0014586
1171	727.93	0.902	0.0120	0.0015136

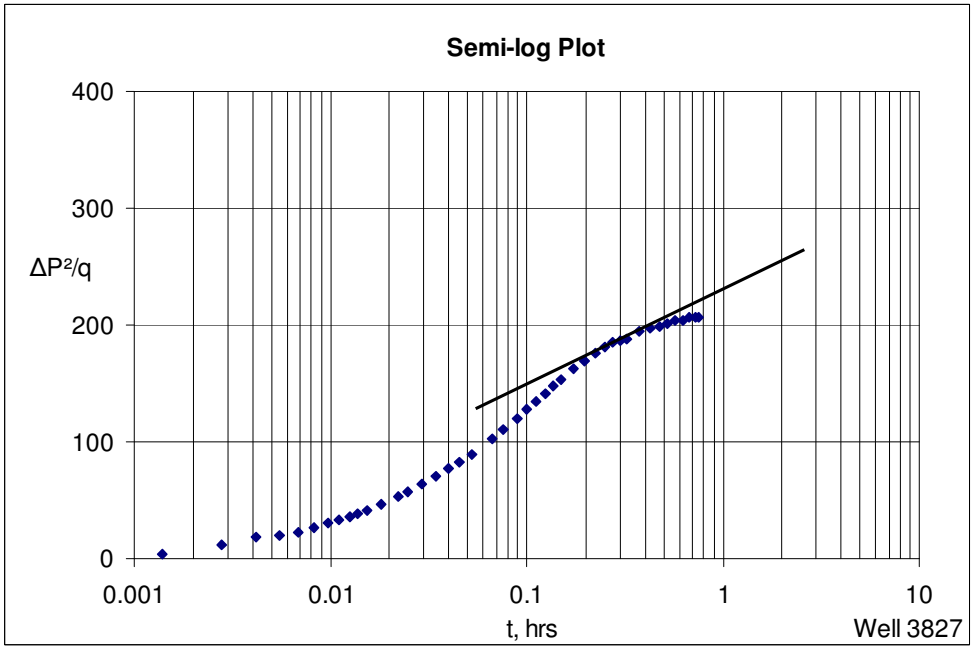

Figure B.4: Drawdown semi-log plot for well 3827, q = 308.32 Mscf

Table B.6: *k* and *S'* for well 3827

q, Mscf	k, mD	S'
308.32	10.01	-2.20
670.26	12.23	-1.61
1171	11.34	-1.52

Table B.7: *D* and *s* for well 3827

D	s	β, 1/ft
7.51×10^{-4}	-2.31	1.87×10^{9}

Well 3931

Table B.8: Gas properties at 75 º F for well 3931

q (Mscf)	$\overline{P}$ (psia)	$\overline{z}$	$\overline{\mu}$ (cp)	$\overline{c}_t$ (psia^{-1})
820.19	957.5	0.874	0.0124	0.0011771
1381.4	901.52	0.881	0.0123	0.001244
2082.39	883.38	0.883	0.0122	0.0012685

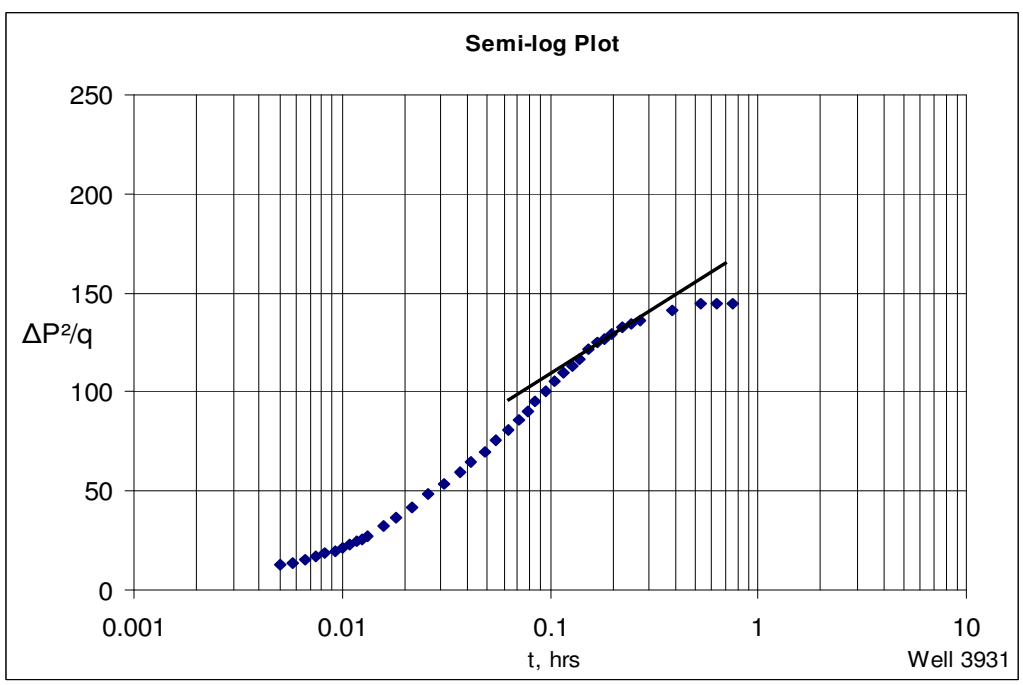

Figure B.5: Drawdown semi-log plot for well 3931, q = 820.19 Mscf

Table B.9: *k* and *S'* for well 3931

q, Mscf	k, mD	S'
820.19	14.59	-2.47
1381.4	12.95	-1.93
2082.39	11.80	-1.60

Table B.10: *D* and *s* for well 3931

D	s	β, 1/ft
6.8×10^{-4}	-2.97	1.48×10^{9}

Well 3870

Table B.11: Gas properties at 75 º F for well 3870

q (Mscf)	$\overline{P}$ (psia)	$\overline{z}$	$\overline{\mu}$ (cp)	$\overline{c}_t$ (psia^{-1})
942.43	1046.55	0.864	0.0126	0.0010845
1639.57	1002.41	0.869	0.0125	0.00113

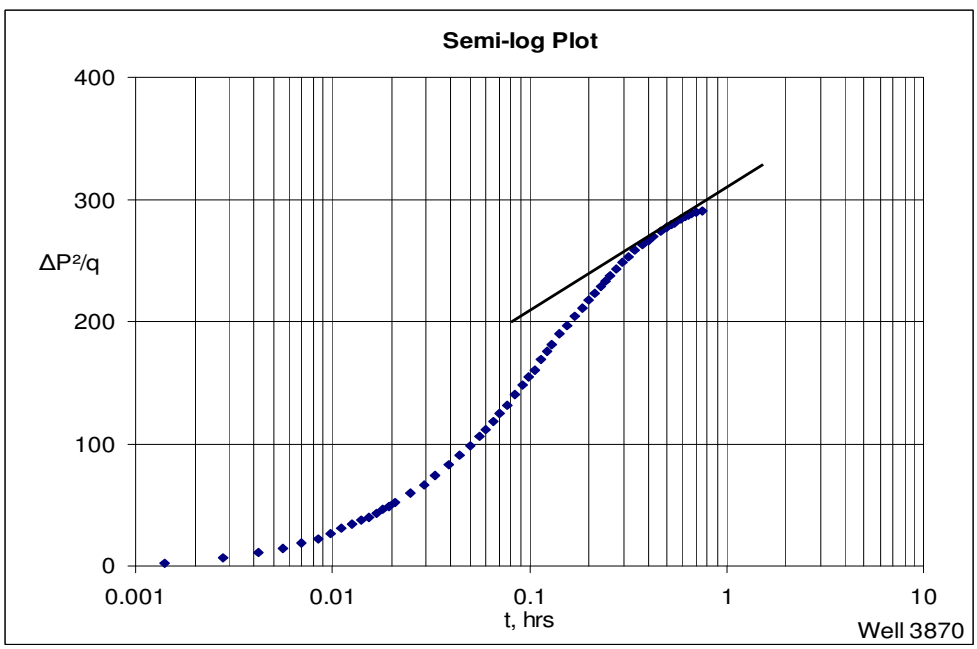

Figure B.6: Drawdown semi-log plot for well 3870, q = 942.43 Mscf

Table B.12: *k* and *S'* for well 3870

q, Mscf	k, mD	S'
942.43	9.65	-1.65
1639.57	11.29	-1.22

Table B.13: *D* and *s* for well 3870

D	s	β, 1/ft
6.17×10^{-4}	-2.23	1.72×10^{9}

Drawdown and Falloff Tests Analysis for Reservoir *B*:

For reservoir *B* one sample calculation is presented. The results of test analysis are tabulated in the following tables:

Well 9096

B14: Gas properties at 79 º F for well 9096

q (Mscf)	$\overline{P}$ (psia)	$\overline{z}$	$\overline{\mu}$ (cp)	$\overline{c}_t$ (psia^{-1})
350	308.83	0.959	0.011176	0.0023610
430	313.75	0.958	0.011183	0.0023247

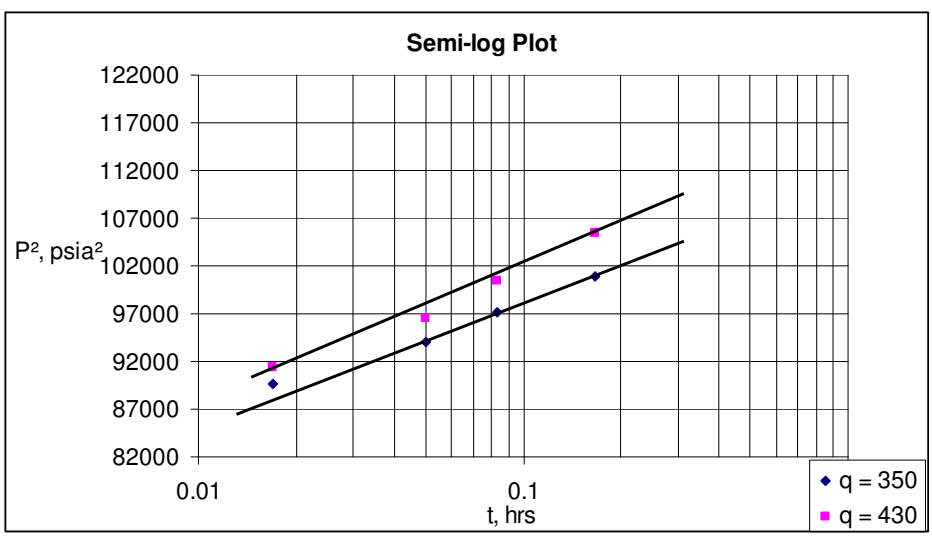

Figure B.7: Drawdown test semi-log plot for well 9096, q = 350 & 430 Mscf

For q = 350 Mscf:

$\left(P_{wf}\right)_{1hr}$ = 109514.5 psia^2

P_{wf} = 85614.76 psia^2

m = 11439.95

$$k = \frac{1637 \times 539 \times 350 \times 0.011176 \times 0.959}{11439.95 \times 50} = 5.79\ mD$$

$$S' = 1.151\left[\frac{109514.5 - 85615.76}{11439.95} - \log\left(\frac{5.79}{0.15 \times 0.011176 \times 0.002361 \times 0.269^2}\right) + 3.23\right]$$

S' = -2.29

Falloff Test:

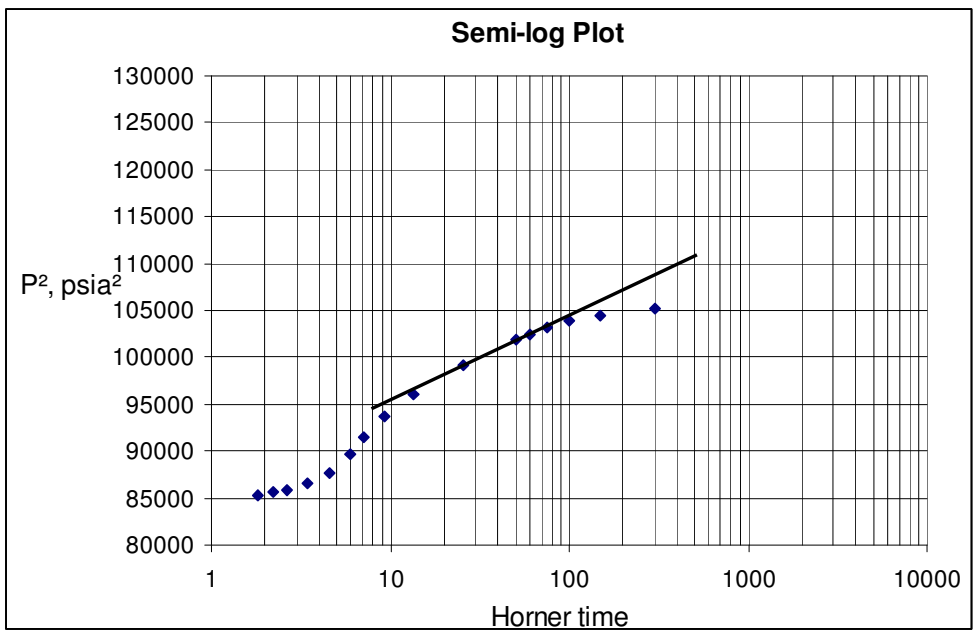

Figure B.8: Falloff test, semi-log plot for well 9096

$\left(P_{ws}\right)_{1hr}$ = 84000 psia^2

m = 16200

$$k = \frac{1637 \times 429.5 \times 539 \times 0.0111765 \times 0.959}{16200 \times 50} = 5.02\ mD$$

$$S' = 1.151\left[\frac{105560 - 84000}{16200} - \log\left(\frac{5.02}{0.15 \times 0.0111765 \times 0.002361 \times 0.269^2}\right) + 3.23\right]$$

S’ = -2.07

From drawdown test results:

Table B.15: *k* and *S’* for well 9096

q, Mscf	k, mD	S’
350	9.65	-1.65
430	11.29	-1.22

Table B.16: *D* and *s* for well 9096

D	s	β, 1/ft
5.0×10^{-4}	-2.46	1.01×10^{10}

<u>Well 7772</u>

Table B.17: Gas properties at 76 º F for well 7772

q (Mscf)	$\overline{P}$ (psia)	$\overline{z}$	$\overline{\mu}$ (cp)	$\overline{c}_t$ (psia^{-1})
2750	301.10	0.959	0.01112	0.0024229
3400	305.33	0.959	0.01113	0.0023925
5203	318.00	0.957	0.01114	0.0022987

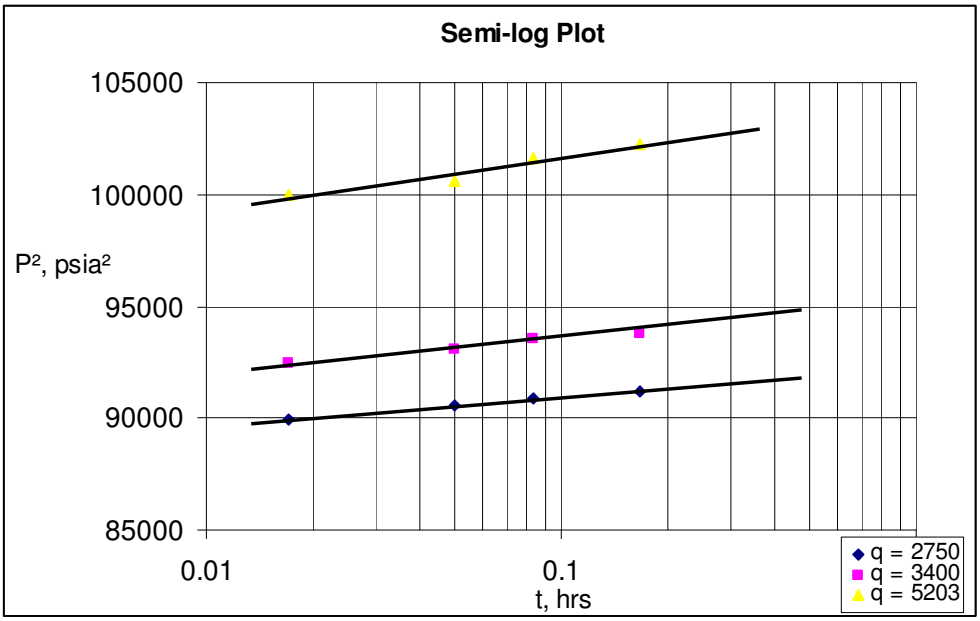

Figure B.9: Drawdown semi-log plot for well 7772, q = 2750, 3400 and 5203 Mscf

Falloff Test:

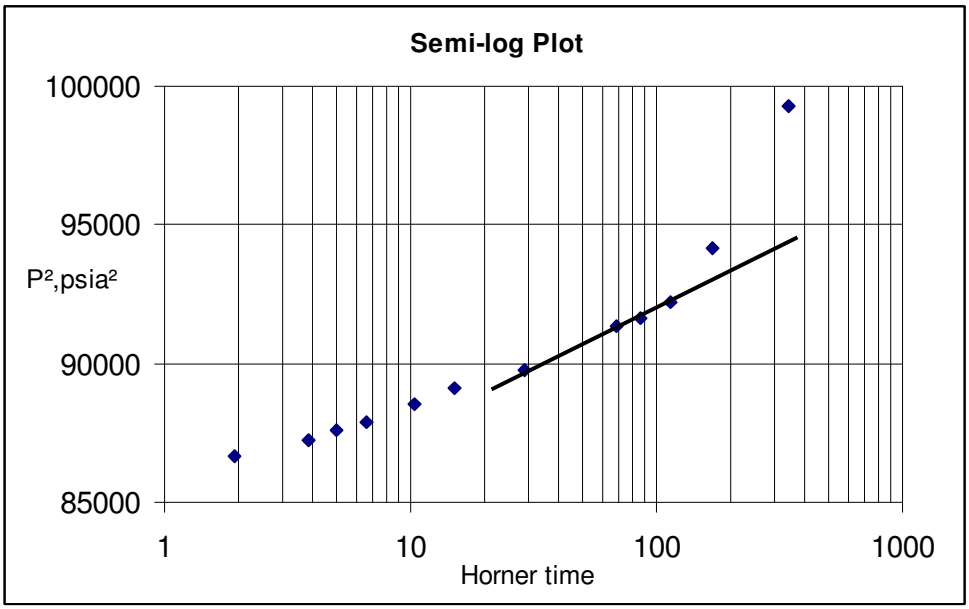

Figure B.10: Falloff test semi-log plot for well 7772

From falloff test: k = 468 mD

S' =1.72

From drawdown test results:

Table B.18: *k* and *S'* for well 7772

q, Mscf	k, mD	S'
2750	498.90	-0.067
3400	573.65	1.1
5203	509.73	1.77

Table B.19: *D* and *s* for well 7772

D	s	β, 1/ft
7.2×10^{-4}	-1.59	9.71×10^{7}

<u>Well 6065</u>

Table B.20: Gas properties at 77 º F for well 6065

q (Mscf)	$\overline{P}$ (psia)	$\overline{z}$	$\overline{\mu}$ (cp)	$\overline{c}_t$ (psia^{-1})
1450	313.53	0.958	0.01115	0.002324
1749	319.55	0.957	0.011161	0.002284
2302	335.85	0.955	0.011182	0.002180

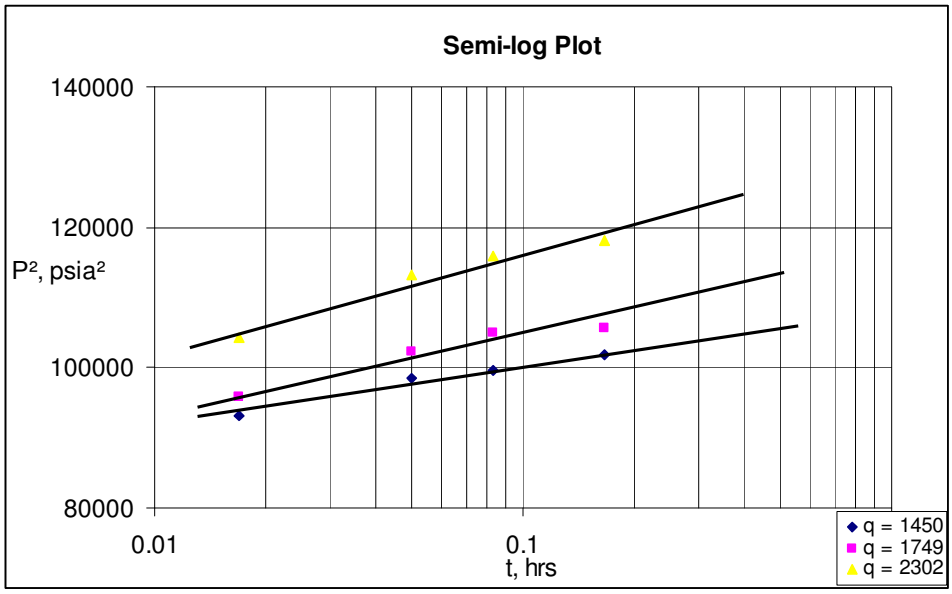

Figure B.11: Drawdown semi-log plot for well 6065, q = 1450, 1749 and 2302 Mscf

Falloff Test:

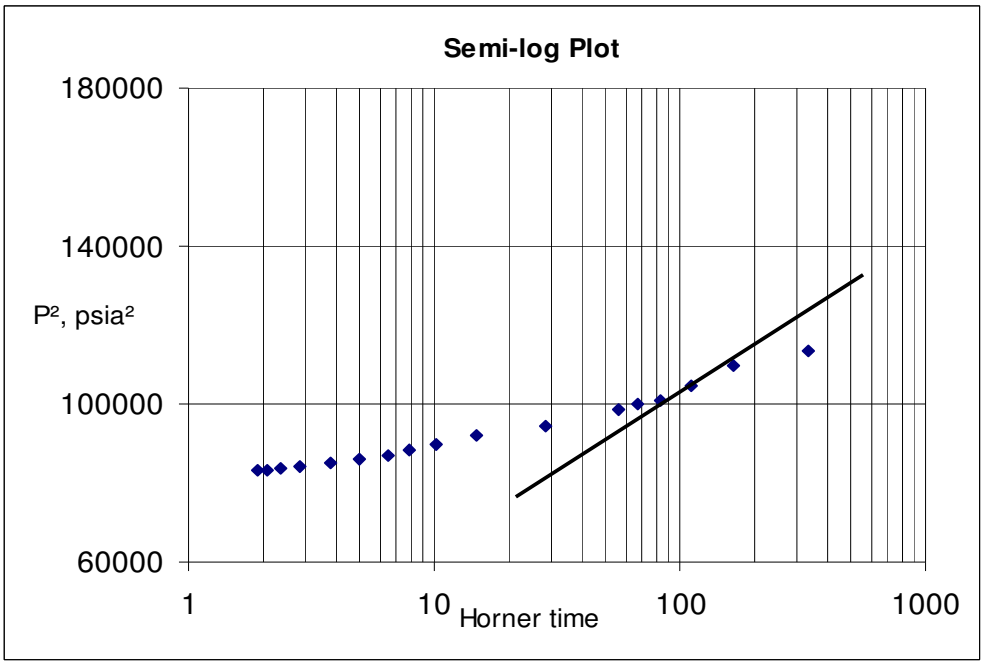

Figure B.12: Falloff test semi-log plot for well 6065

k = 31.78

S' = -2.31

From drawdown test results:

Table B.21: *k* and *S'* for well 6065

q, Mscf	k, mD	S'
1450	31.23	-2.40
1749	31.54	-2.38
2302	30.44	-2.38

Table B.22: *D* and *s* for well 6065

D	s	β, 1/ft
5.82×10^{-4}	-3.25	1.69×10^{9}

APPENDIX C

EVALUATE EXISTING *β* CORRRELATIONS AND DEVELOP *β* CORRRELATION FOR RESEVOIR *A* AND *B*

β Correlations Evaluation for Reservoir *A*

For each well, one flow rate was selected and *β* correlations were evaluated. Results are tabulated in the following tables:

Table C.1: *β* correlations evaluation for well 3585 and flow rate 2320.43 Mscf

Q = 2320.43 Mscf	β	$s_{equation}$	s_{test}	Error %
Geertsma	7.727E+07	-2.20	-3.1	27.87
Thauvin & Mohant	8.427E+06	-2.16	-3.1	29.04
Janicek & Katz	1.363E+09	-2.74	-3.1	10.04
Jones	1.759E+09	-2.87	-3.1	5.79
Jones	1.686E+09	-2.83	-3.1	7.21
Coles & Hartman	5.642E+09	-4.23	-3.1	-38.55
Coles & Hartman	1.361E+09	-2.67	-3.1	12.47
Svec & Engler	2.515E+08	-2.27	-3.1	25.42
Pascal et al	9.770E+10	-44.79	-3.1	-1368.50
Tek et al	1.439E+09	-2.78	-3.1	8.72

Table C.2: β correlations evaluation for well 3946 and flow rate 1363.1 Mscf

Q = 1363.1 Mscf	β	$s_{equation}$	s_{test}	Error %
Geertsma	4.950E+07	-2.62	-3.6	27.83
Thauvin & Mohant	5.398E+06	-2.57	-3.6	29.29
Janicek & Katz	4.477E+08	-3.10	-3.6	14.58
Jones	4.749E+08	-3.13	-3.6	13.67
Jones	4.238E+08	-3.07	-3.6	15.37
Coles & Hartman	1.057E+09	-3.84	-3.6	-5.70
Coles & Hartman	2.762E+08	-2.89	-3.6	20.28
Svec & Engler	1.032E+08	-2.68	-3.6	26.04
Pascal et al	3.427E+10	-43.95	-3.6	-1110.83
Tek et al	4.941E+08	-3.16	-3.6	13.04

Table C.3: β correlations evaluation for well 3827 and flow rate 1171 Mscf

Q = 1171 Mscf	β	$s_{equation}$	s_{test}	Error %
Geertsma	7.321E+07	-1.56	-2.3	32.67
Thauvin & Mohant	7.985E+06	-1.52	-2.3	34.03
Janicek & Katz	1.191E+09	-2.09	-2.3	9.33
Jones	1.501E+09	-2.24	-2.3	2.86
Jones	1.426E+09	-2.21	-2.3	4.42
Coles & Hartman	4.606E+09	-3.74	-2.3	-61.97
Coles & Hartman	1.122E+09	-2.06	-2.3	10.78
Svec & Engler	2.258E+08	-1.63	-2.3	29.48
Pascal et al	8.606E+10	-43.02	-2.3	-1762.51
Tek et al	1.264E+09	-2.13	-2.3	7.80

Table C.4: β correlations evaluation for well 3931 and flow rate 2082.39 Mscf

Q = 2082.39 Mscf	β	$s_{equation}$	s_{test}	Error %
Geertsma	7.177E+07	-1.66	-3.0	44.02
Thauvin & Mohant	7.828E+06	-1.61	-3.0	45.90
Janicek & Katz	1.133E+09	-2.59	-3.0	12.89
Jones	1.416E+09	-2.83	-3.0	4.61
Jones	1.341E+09	-2.77	-3.0	6.80
Coles & Hartman	4.274E+09	-5.32	-3.0	-79.21
Coles & Hartman	1.045E+09	-2.51	-3.0	15.49
Svec & Engler	2.170E+08	-1.79	-3.0	39.76
Pascal et al	8.212E+10	-73.12	-3.0	-2362.07
Tek et al	1.205E+09	-2.65	-3.0	10.78

Table C.5: β correlations evaluation for well 3870 and flow rate 1639.57 Mscf

Q = 1639.57 Mscf	β	$s_{equation}$	s_{test}	Error %
Geertsma	7.337E+07	-1.27	-2.2	43.18
Thauvin & Mohant	8.002E+06	-1.22	-2.2	45.06
Janicek & Katz	1.198E+09	-1.99	-2.2	10.87
Jones	1.511E+09	-2.19	-2.2	1.86
Jones	1.436E+09	-2.14	-2.2	4.01
Coles & Hartman	4.644E+09	-4.20	-2.2	-88.19
Coles & Hartman	1.131E+09	-1.94	-2.2	12.79
Svec & Engler	2.268E+08	-1.36	-2.2	38.77
Pascal et al	8.650E+10	-56.66	-2.2	-2440.95
Tek et al	1.271E+09	-2.03	-2.2	8.76

β* Correlations Evaluation for Reservoir *B

For each well, one flow rate was selected and *β* correlations were evaluated. Results are tabulated in the following tables:

Table C.6: *β* correlations evaluation for well 9096 and flow rate 350 Mscf

Q = 350 Mscf	β	$s_{equation}$	s_{test}	Error %
Geertsma	7.011E+07	-2.29	-2.5	7.05
Thauvin & Mohant	1.008E+07	-2.29	-2.5	7.09
Janicek & Katz	2.621E+09	-2.34	-2.5	5.25
Jones	3.888E+09	-2.36	-2.5	4.36
Jones	4.043E+09	-2.36	-2.5	4.25
Coles & Hartman	1.681E+10	-2.58	-2.5	-4.74
Coles & Hartman	3.878E+09	-2.36	-2.5	4.37
Svec & Engler	4.128E+08	-2.30	-2.5	6.81
Pascal et al	1.897E+11	-5.58	-2.5	-126.49
Tek et al	2.832E+09	-2.34	-2.5	5.10

Table C.7: *β* correlations evaluation for well 7772 and flow rate 3400 Mscf

Q = 3400 Mscf	β	$s_{equation}$	s_{test}	Error %
Geertsma	7.043E+06	0.9	-1.6	156.93
Thauvin & Mohant	1.012E+06	1.07	-1.6	167.42
Janicek & Katz	8.384E+06	0.87	-1.6	154.60
Jones	4.525E+06	0.97	-1.6	161.31
Jones	3.258E+06	1.01	-1.6	163.51
Coles & Hartman	2.973E+06	1.02	-1.6	164.01
Coles & Hartman	1.037E+06	1.07	-1.6	167.38
Svec & Engler	4.166E+06	0.98	-1.6	161.94
Pascal et al	8.528E+08	-22.49	-1.6	-1314.38
Tek et al	1.140E+07	0.78	-1.6	149.35

Table C.8: β correlations evaluation for well 6065 and flow rate 2302 Mscf

Q = 2302 Mscf	β	$s_{equation}$	s_{test}	Error %
Geertsma	3.058E+07	-1.98	-3.3	40.24
Thauvin & Mohant	4.394E+06	-1.96	-3.3	40.86
Janicek & Katz	3.292E+08	-2.22	-3.3	33.12
Jones	3.390E+08	-2.23	-3.3	32.89
Jones	3.087E+08	-2.20	-3.3	33.61
Coles & Hartman	7.423E+08	-2.55	-3.3	23.28
Coles & Hartman	1.988E+08	-2.12	-3.3	36.23
Svec & Engler	7.851E+07	-2.02	-3.3	39.09
Pascal et al	2.694E+10	-23.27	-3.3	-601.05
Tek et al	3.866E+08	-2.26	-3.3	31.75

Develop β Correlation for Reservoir *A*:

The value of β for each well was presented in Appendix B. By plotting β versus well permeability on the log-log paper, β correlation for reservoir *A* was developed. Table C.9 summarizes *k* and β and their logarithmic values for the wells in reservoir *A*.

Table C.9: k and β for wells in reservoir *A*

Well	k, mD	β, 1/ft	log*k*	log β
3946	23.615	9.28E+08	1.37E+00	8.968
3827	11.19	1.87E+09	1.05E+00	9.272
3931	13.11	1.48E+09	1.12E+00	9.170
3870	10.47	1.72E+09	1.02E+00	9.236
3585	12.52	1.61E+09	1.10E+00	9.207

SUMMARY OUTPUT (Microsoft Excel)

Regression Statistics						
Multiple R	0.983198046					
R Square	0.966678398					
Adjusted R Square	0.950017597					
Standard Error	0.03042564					
Observations	4					
ANOVA						
	df	*SS*	*MS*	*F*	*Significance F*	
Regression	1	0.05371129	0.05371129	58.02112354	0.01680195	
Residual	2	0.001851439	0.00092572			
Total	3	0.05556273				
	Coefficients	*Standard Error*	*t Stat*	*P-value*	*Lower 95%*	*Upper 95%*
Intercept	10.11511266	0.125444566	80.60893332	0.000153863	9.57220826	10.65169707
X Variable 1	-0.83505674	0.109234513	-7.617159808	0.016801954	-1.3020549	-0.36205857

$$\beta = \frac{1\times 10^{10.115}}{k^{0.835}}$$

Using the new β correlation for reservoir A, β was determine for each well and they were compared with β values obtained from multi-rate tests analysis to measure the generated error. One sample calculation is presented here. Table C.10 summarizes the comparison of β values from 2 methods.

<u>Well 3585</u>

$$\beta = \frac{1\times 10^{10.115}}{12.52^{0.835}} = 1.57\times 10^{9}\ \text{1/ft}$$

Table C.10: Comparison of β from 2 methods

Well	β, 1/ft (Test)	β, 1/ft (Equation 41)	Error (%)
3946	9.33E+08	9.71E+08	0.4
3827	1.87E+09	1.78E+09	5.0
3931	1.48E+09	1.51E+09	2.1
3870	1.72E+09	1.82E+09	5.7
3585	1.61E+09	1.57E+09	2.3

Develop β Correlation for Reservoir *B*:

The value of β for each well was presented in Appendix B. By plotting β versus well permeability on the log-log paper, β correlation for reservoir *B* was developed. Table C.11 summarizes *k* and β and their logarithmic values for the wells in reservoir *B*.

Table C.11: k and β for wells in reservoir *B*

Well	k, mD	β, 1/ft	log*k*	log *β*
9096	23.615	1.01E+10	1.373188	10.005
7772	11.19	9.71E+07	1.04883	7.987
6065	13.11	1.69E+09	1.117603	9.227

SUMMARYOUTPUT

Regression Statistics	
Multiple R	0.992455449
R Square	0.984967819
Adjusted R Square	0.979957092
Standard Error	0.095393656
Observations	5
ANOVA	

	df	*SS*	*MS*	*F*	*Significance F*	
Regression	1	1.788793812	1.788793812	196.571837	0.000785763	
Residual	3	0.027299849	0.00909995			
Total	4	1.81609366				
	Coefficients	*Standard Error*	*t Stat*	*P-value*	*Lower 95%*	*Upper 95%*
Intercept	10.79016692	0.078055714	128.2182483	1.04599E-06	9.7597588	10.25657504
X Variable 1	-1.02936979	0.054375721	-14.02040788	0.000785763	-0.935417599	-0.58932197

$$\beta = \frac{1\times 10^{10.79}}{k^{1.029}}$$

Using the new β correlation for reservoir B, β was determine for each well and they were compared with β values obtained from multi-rate tests analysis to measure the generated error. One sample calculation is presented here. Table C.12 summarizes the comparison of β values from 2 methods.

Well 7772

$$\beta = \frac{1\times10^{10.79}}{12.52^{1.029}} = 9.71\times10^{7}\ \text{1/ft}$$

Table C.12: Comparison of β from 2 methods

Well	β, 1/ft (Test)	β, 1/ft (Equation 42)	Error (%)
9096	1.012×10^{10}	1.01×10^{10}	0.0
7772	9.71×10^{7}	9.71×10^{7}	0.0
6065	1.685×10^{9}	1.76×10^{9}	4.0

APPENDIX D

DELIVERABILITY EQUATION DETERMINATION

In order to see how deliverability equation is determined for a well using the new correlation developed for reservoir *A*, One sample calculation is carried out using equation (41).

Deliverability equation determination for well 3946 and flow rate of 2002.64 Mscf using equation (41) is performed as follows:

1) $\beta = \dfrac{1\times10^{10.115}}{22.42^{0.835}} = 9.71\times10^{8}$ 1/ft

2) $D = \dfrac{2.22\times10^{-15}\times0.58\times22.42\times9.71\times10^{8}}{0.012076\times10\times0.3} = 7.73\times10^{-4}$

From well tests analysis S' = -2.06 (see Appendix *B*)

3) s = -2.06 - ($7.73\times10^{-4}\times2002.64$) = -3.61

Using equation (23)

4) $A = \dfrac{1637\times535\times0.01208\times0.89}{22.42\times10}\left[\log\left(\dfrac{22.42\times0.5403}{0.14\times0.01208\times0.00136\times0.3^{2}}\right)-3.23+(0.87\times-3.61)\right]$

A = 58.65

Using equation (24)

5) $B = \dfrac{3.161\times10^{-12}\times9.71\times10^{8}\times0.58\times0.89\times535}{0.3\times10^{2}} = 0.0283$

6) $\overline{P}_R^2 - P_{wf}^2 = 58.65q + 0.0283q^2$

Now that we have deliverability equation for well 3946, one can calculate reservoir average pressure at any point of time.

From Table A.2:

When t = 0.5403 hrs $P_{wf} = 760.14$ psia

$$\overline{P}_R^2 - 760.14^2 = (58.65 \times 2002.64) + (0.0283 \times 2002.64^2)$$

$$\overline{P}_R = 900 \text{ psia}$$

The same procedure is applied to determine well deliverability equation for reservoir *B*. Deliverability equation determination for well 6065 and flow rate of 1450 Mscf using equation (42) is performed as follows:

1) $\beta = \dfrac{1 \times 10^{10.79}}{31.23^{1.029}} = 1.76 \times 10^9$ 1/ft

2) $D = \dfrac{2.22 \times 10^{-15} \times 0.58 \times 31.23 \times 1.76 \times 10^9}{0.011153234 \times 50 \times 0.204} = 6.317 \times 10^{-4}$

From well testing analysis S' = -2.4 (see Appendix *B*)

3) s = -2.4 - ($6.317 \times 10^{-4} \times 1450$) = -3.316

Using equation (23)

4) $A = \dfrac{1637 \times 537 \times 0.011153 \times 0.958}{31.23 \times 50}\left[\log\left(\dfrac{31.23 \times 0.167}{0.15 \times 0.011153 \times 0.00233 \times 0.204^2}\right) - 3.23 + (0.87 \times -3.316)\right]$

A = 8.38

Using equation (24)

5) $B = \dfrac{3.161 \times 10^{-12} \times 1.76 \times 10^9 \times 0.58 \times 0.958 \times 537}{0.269 \times 50^2} = 0.0033$

6) $\overline{P}_R^2 - P_{wf}^2 = 8.38q + 0.003q^2$

Now that we have deliverability equation for well 6065, one can calculate reservoir average pressure at any point of time.

From Table A.10:

When t = 0.167 hrs P_{wf} = 319.3 psia

$$\overline{P}_R^2 - 319.3^2 = (8.38 \times 1450) + (0.003 \times 1450^2)$$

$\overline{P}_R$ = 348 psia